Electronic Supplementary Material (ESI) for Journal of Materials Chemistry C.
This journal is © The Royal Society of Chemistry 2019

Supporting Information

Salt–cocrystal continuum for photofunction modulation: Stimuli-responsive fluorescence color-tuning of pyridine-modified intramolecular charge–transfer dyes and acid complexes

Yoshio Yano, Toshikazu Ono,* Sou Hatanaka, Daniel T. Gryko, and Yoshio Hisaeda*

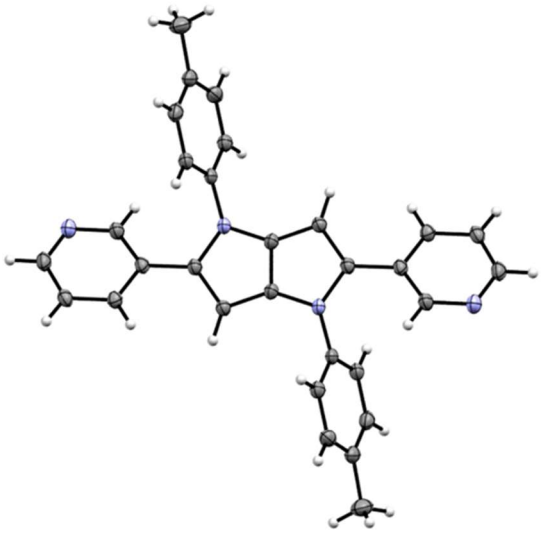

Fig. S1 Crystal structure of **1** (123 K). Ellipsoids are plotted at the 50% probability level.

Table S1 Crystallographic data for **1** (123 K).

Compound	**1**
CCDC No.	1910438
empirical formula	$C_{30}H_{24}N_4$
formula weight	440.53
temperature [K]	123
wavelength [Å]	0.71073
crystal system	triclinic
space group	P -1
a [Å]	6.0824(4)
b [Å]	7.1390(7)
c [Å]	13.6977(15)
α [°]	89.603(8)
β [°]	77.345(8)
γ [°]	82.266(7)
Volume [Å^3]	574.90(9)
Z	1
Density (calculated) [g/cm^3]	1.272
Absorption coefficient [mm^{-1}]	0.076
F(000)	232.0
θ [°]	2.880 to 26.368
Reflections collected	3846
Independent reflections	2335 [$R_{(int)}$ = 0.0199]
Data / restraints / parameters	2335 / 0 / 155
Goodness-of-fit on F^2	0.989
$R1$[a] [$I>2\sigma(I)$]	0.0456
$wR2$ [b] (all data)	0.1377
Largest diff. peak and hole [e.Å^{-3}]	0.24 and -0.25

a: $R1= (\sum||F_o|-|F_c||)/(\sum|F_o|)$. b: $wR2= [\sum w(F_o^2-F_c^2)^2/\sum wF_o^4]^{1/2}$, where $w= 1/[\sigma^2(F_o^2)+(0.0900 (F_o^2+2F_c^2)/3)^2+ 0.1400 (F_o^2+2F_c^2)/3]$

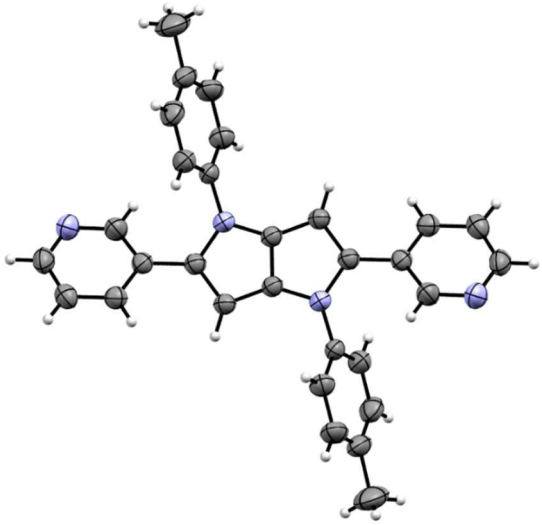

Fig. S2 Crystal structure of **1** (298 K). Ellipsoids are plotted at the 50% probability level.

Table S2 Crystallographic data for **1** (298 K).

Compound	**1**
CCDC No.	1910439
empirical formula	$C_{30}H_{24}N_4$
formula weight	440.53
temperature [K]	298
wavelength [Å]	0.71073
crystal system	triclinic
space group	P -1
a [Å]	6.1699(4)
b [Å]	7.2595(5)
c [Å]	13.6139(8)
α [°]	89.162(5)
β [°]	79.508(5)
γ [°]	80.710(5)
Volume [Å^3]	591.64(7)
Z	1
Density (calculated) [g/cm^3]	1.236
Absorption coefficient [mm^{-1}]	0.074
F(000)	232.0
θ [°]	2.843 to 26.370
Reflections collected	6300
Independent reflections	2412 [$R_{(int)}$ = 0.0169]
Data / restraints / parameters	2412 / 0 / 155
Goodness-of-fit on F^2	1.036
$R1$[a] [$I>2\sigma(I)$]	0.0381
$wR2$ [b] (all data)	0.1098
Largest diff. peak and hole [e.Å^{-3}]	0.17 and -0.17

a: $R1= (\sum||F_o|-|F_c||)/(\sum|F_o|)$. b: $wR2= [\sum w(F_o^2-F_c^2)^2/\sum wF_o^4]^{1/2}$, where $w= 1/[\sigma^2(F_o^2)+(0.0520 (F_o^2+2F_c^2)/3)^2+ 0.1050 (F_o^2+2F_c^2)/3]$

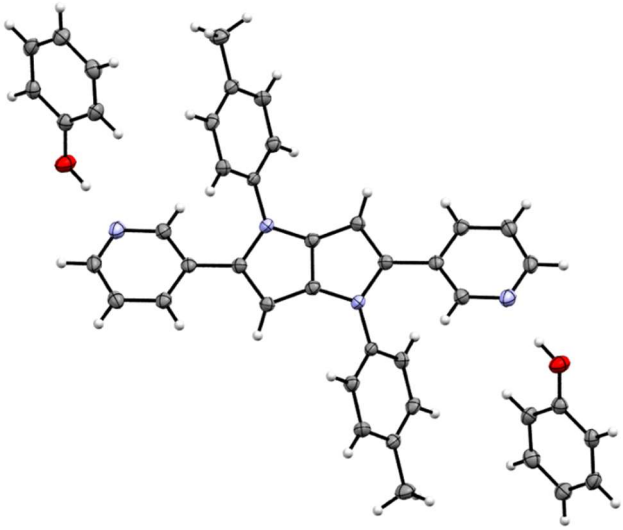

Fig. S3 Crystal structure of **1•a** (123 K). Ellipsoids are plotted at the 50% probability level.

Table S3 Crystallographic data for **1•a** (123 K).

Compound	**1•a**
CCDC No.	1910440
empirical formula	$C_{42}H_{36}N_4O_2$
formula weight	628.75
temperature [K]	123
wavelength [Å]	0.71073
crystal system	triclinic
space group	P -1
a [Å]	8.8912(5)
b [Å]	9.5438(6)
c [Å]	10.6502(7)
α [°]	93.787(5)
β [°]	91.373(5)
γ [°]	112.630(6)
Volume [Å^3]	831.13(10)
Z	1
Density (calculated) [g/cm^3]	1.256
Absorption coefficient [mm^{-1}]	0.078
F(000)	332.0
θ [°]	2.663 to 26.366
Reflections collected	8591
Independent reflections	3388 [$R_{(int)}$ = 0.0199]
Data / restraints / parameters	3388 / 0 / 222
Goodness-of-fit on F^2	0.999
$R1^a$ [$I>2\sigma(I)$]	0.0414
$wR2^b$ (all data)	0.1030
Largest diff. peak and hole [e.Å^{-3}]	0.20 and -0.24

a: $R1 = (\sum||F_o|-|F_c||)/(\sum|F_o|)$. b: $wR2 = [\sum w(F_o^2-F_c^2)^2/\sum wF_o^4]^{1/2}$, where $w = 1/[\sigma^2(F_o^2)+(0.0430\ (F_o^2+2F_c^2)/3)^2+ 0.1380\ (F_o^2+2F_c^2)/3]$

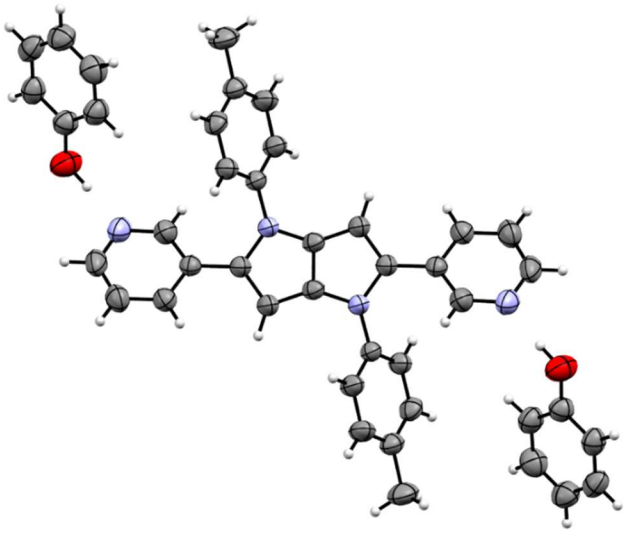

Fig. S4 Crystal structure of **1•a** (298 K). Ellipsoids are plotted at the 50% probability level.

Table S4 Crystallographic data for **1•a** (298 K).

Compound	**1•a**
CCDC No.	1910441
empirical formula	$C_{42}H_{36}N_4O_2$
formula weight	628.75
temperature [K]	298
wavelength [Å]	0.71073
crystal system	triclinic
space group	P -1
a [Å]	8.9338(7)
b [Å]	9.6930(8)
c [Å]	10.7136(8)
α [°]	93.146(6)
β [°]	90.933(6)
γ [°]	112.034(7)
Volume [Å^3]	858.01(12)
Z	1
Density (calculated) [g/cm^3]	1.217
Absorption coefficient [mm^{-1}]	0.076
F(000)	332.0
θ [°]	2.647 to 26.367
Reflections collected	7709
Independent reflections	3502 [$R_{(int)}$ = 0.0331]
Data / restraints / parameters	3502 / 0 / 222
Goodness-of-fit on F^2	1.006
$R1$[a] [$I>2\sigma(I)$]	0.0510
$wR2$ [b] (all data)	0.1420
Largest diff. peak and hole [e.Å^{-3}]	0.15 and -0.17

a: $R1 = (\sum||F_o|-|F_c||)/(\sum|F_o|)$. b: $wR2 = [\sum w(F_o^2-F_c^2)^2/\sum wF_o^4]^{1/2}$, where $w = 1/[\sigma^2(F_o^2)+(0.0470(F_o^2+2F_c^2)/3)^2]$

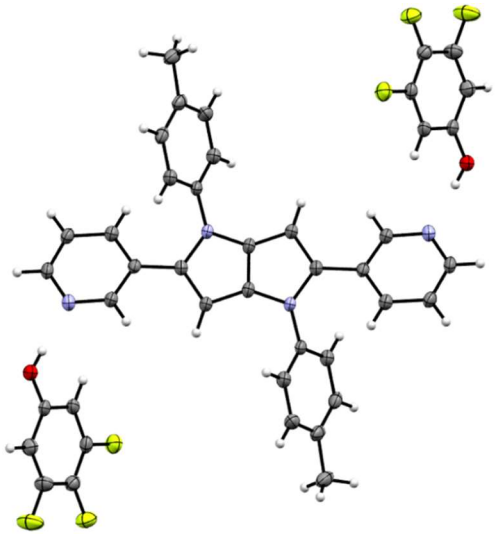

Fig. S5 Crystal structure of **1•b** (123 K). Ellipsoids are plotted at the 50% probability level.

Table S5 Crystallographic data for **1•b** (123 K).

Compound	**1•b**
CCDC No.	1910442
empirical formula	$C_{42}H_{30}F_6N_4O_2$
formula weight	736.70
temperature [K]	123
wavelength [Å]	0.71073
crystal system	triclinic
space group	P -1
a [Å]	7.2393(5)
b [Å]	10.9716(9)
c [Å]	11.9913(11)
α [°]	70.492(8)
β [°]	72.988(7)
γ [°]	88.835(6)
Volume [Å^3]	855.30(13)
Z	1
Density (calculated) [g/cm^3]	1.430
Absorption coefficient [mm^{-1}]	0.112
F(000)	380.0
θ [°]	2.953 to 26.37
Reflections collected	11526
Independent reflections	3485 [$R_{(int)}$ = 0.0357]
Data / restraints / parameters	3485 / 0 / 246
Goodness-of-fit on F^2	1.046
$R1$[a] [$I>2\sigma(I)$]	0.0546
$wR2$ [b] (all data)	0.1603
Largest diff. peak and hole [e.Å^{-3}]	0.36 and -0.39

a: $R1= (\sum||F_o|-|F_c||)/(\sum|F_o|)$. b: $wR2= [\sum w(F_o^2-F_c^2)^2/\sum wF_o^4]^{1/2}$, where $w= 1/[\sigma^2(F_o^2)+(0.0970\ (F_o^2+2F_c^2)/3)^2+ 0.3200\ (F_o^2+2F_c^2)/3]$

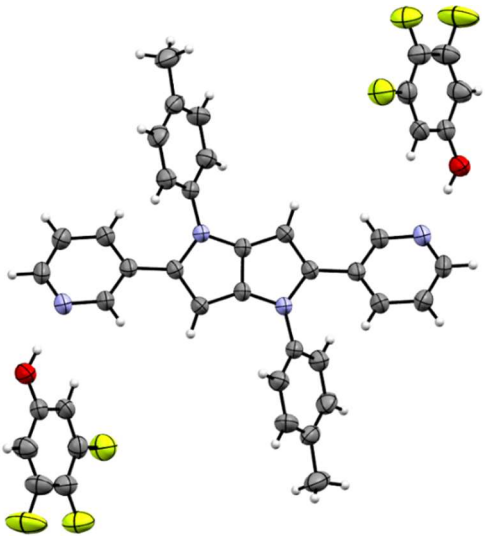

Fig. S6 Crystal structure of **1•b** (298 K). Ellipsoids are plotted at the 50% probability level.

Table S6 Crystallographic data for **1•b** (298 K).

Compound	**1•b**
CCDC No.	1910443
empirical formula	$C_{42}H_{30}F_6N_4O_2$
formula weight	736.70
temperature [K]	298
wavelength [Å]	0.71073
crystal system	triclinic
space group	P -1
a [Å]	7.3705(6)
b [Å]	11.0005(12)
c [Å]	12.0029(13)
α [°]	109.130(10)
β [°]	106.773(8)
γ [°]	90.454(8)
Volume [Å^3]	874.66(16)
Z	1
Density (calculated) [g/cm^3]	1.399
Absorption coefficient [mm^{-1}]	0.109
F(000)	380.0
θ [°]	2.905 to 26.373
Reflections collected	7431
Independent reflections	3571 [$R_{(int)}$ = 0.0366]
Data / restraints / parameters	3571 / 0 / 249
Goodness-of-fit on F^2	1.067
$R1$[a] [$I>2\sigma(I)$]	0.0578
$wR2$ [b] (all data)	0.1729
Largest diff. peak and hole [e.Å^{-3}]	0.23 and -0.26

a: $R1= (\sum||F_o|-|F_c||)/(\sum|F_o|)$. b: $wR2= [\sum w(F_o^2-F_c^2)^2/\sum wF_o^4]^{1/2}$, where $w= 1/[\sigma^2(F_o^2)+(0.0868(F_o^2+2F_c^2)/3)^2+0.1906(F_o^2+2F_c^2)/3]$

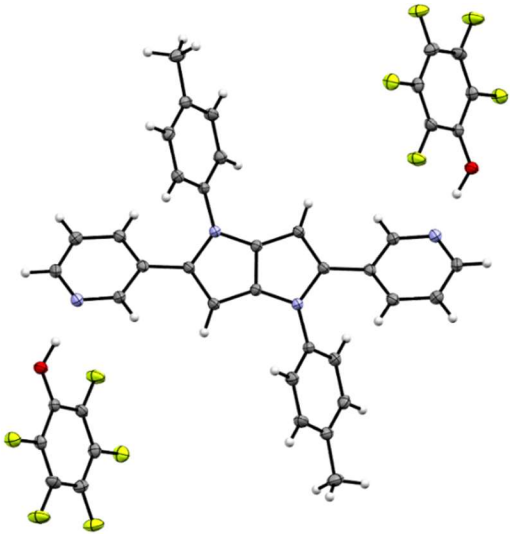

Fig. S7 Crystal structure of **1•c** (123 K). Ellipsoids are plotted at the 50% probability level.

Table S7 Crystallographic data for **1•c** (123 K).

Compound	**1•c**
CCDC No.	1910444
empirical formula	$C_{42}H_{26}F_{10}N_4O_2$
formula weight	808.67
temperature [K]	123
wavelength [Å]	0.71073
crystal system	triclinic
space group	P -1
a [Å]	7.1878(5)
b [Å]	11.3276(9)
c [Å]	12.0753(8)
α [°]	109.633(7)
β [°]	106.637(6)
γ [°]	90.162(6)
Volume [Å^3]	881.90(12)
Z	1
Density (calculated) [g/cm^3]	1.523
Absorption coefficient [mm^{-1}]	0.131
F(000)	412.0
θ [°]	2.976 to 26.37
Reflections collected	6129
Independent reflections	3562 [$R_{(int)}$ = 0.0141]
Data / restraints / parameters	3562 / 0 / 267
Goodness-of-fit on F^2	0.987
$R1$[a] [$I>2\sigma(I)$]	0.0346
$wR2$ [b] (all data)	0.1006
Largest diff. peak and hole [e.Å^{-3}]	0.27 and -0.23

a: $R1= (\sum||F_o|-|F_c||)/(\sum|F_o|)$. b: $wR2= [\sum w(F_o^2-F_c^2)^2/\sum wF_o^4]^{1/2}$, where $w= 1/[\sigma^2(F_o^2)+(0.0550(F_o^2+2F_c^2)/3)^2+ 0.3710(F_o^2+2F_c^2)/3]$

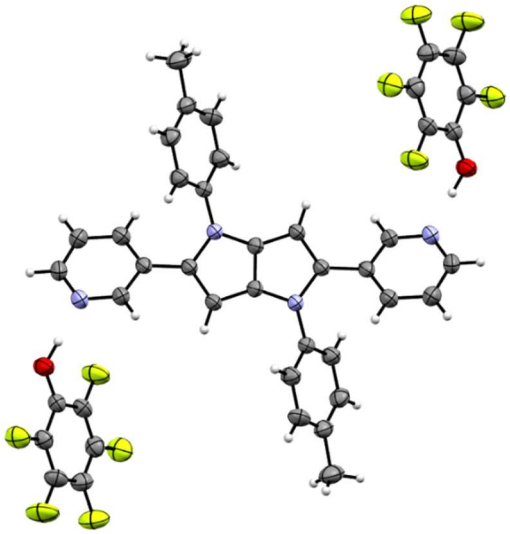

Fig. S8 Crystal structure of **1•c** (298 K). Ellipsoids are plotted at the 50% probability level.

Table S8 Crystallographic data for **1•c** (298 K).

Compound	**1•c**
CCDC No.	1910445
empirical formula	$C_{42}H_{26}F_{10}N_4O_2$
formula weight	808.67
temperature [K]	298
wavelength [Å]	0.71073
crystal system	triclinic
space group	P -1
a [Å]	7.3417(4)
b [Å]	11.3589(7)
c [Å]	12.1244(7)
α [°]	109.165(5)
β [°]	106.484(5)
γ [°]	91.817(5)
Volume [Å^3]	907.06(10)
Z	1
Density (calculated) [g/cm^3]	1.480
Absorption coefficient [mm^{-1}]	0.128
F(000)	412.0
θ [°]	2.921 to 26.372
Reflections collected	8137
Independent reflections	3695 [$R_{(int)}$ = 0.0139]
Data / restraints / parameters	3695 / 0 / 267
Goodness-of-fit on F^2	1.019
$R1$[a] [$I>2\sigma(I)$]	0.0387
$wR2$ [b] (all data)	0.116
Largest diff. peak and hole [e.Å^{-3}]	0.17 and -0.18

a: $R1= (\sum||F_o|-|F_c||)/(\sum|F_o|)$. b: $wR2= [\sum w(F_o^2-F_c^2)^2/\sum wF_o^4]^{1/2}$, where $w= 1/[\sigma^2(F_o^2)+(0.0530(F_o^2+2F_c^2)/3)^2+ 0.2440(F_o^2+2F_c^2)/3]$

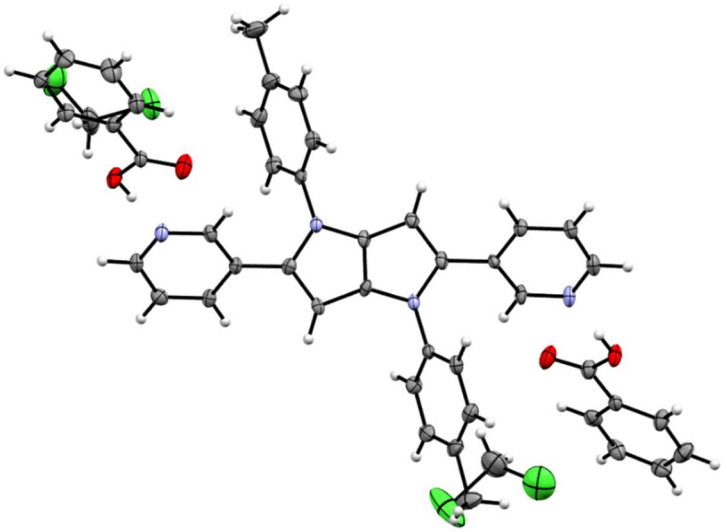

Fig. S9 Crystal structure of **1•d**⊃CH_2Cl_2 (123 K). Ellipsoids are plotted at the 50% probability level.

Table S9 Crystallographic data for **1•d**⊃CH_2Cl_2 (123 K**).**

Compound	**1•d**⊃CH_2Cl_2
CCDC No.	1910446
empirical formula	$C_{46}H_{40}Cl_4N_4O_4$
formula weight	854.62
temperature [K]	123
wavelength [Å]	0.71073
crystal system	orthorhombic
space group	$Pna2_1$
a [Å]	24.062(2)
b [Å]	6.2048(7)
c [Å]	27.631(3)
α [°]	90
β [°]	90
γ [°]	90
Volume [Å^3]	4125.3(7)
Z	4
Density (calculated) [g/cm^3]	1.376
Absorption coefficient [mm^{-1}]	0.337
F(000)	1776.0
θ [°]	2.785 to 26.372
Reflections collected	13766
Independent reflections	7325 [$R_{(int)}$ = 0.0424]
Data / restraints / parameters	7325 / 1 / 530
Goodness-of-fit on F^2	1.139
$R1$[a] [$I>2\sigma(I)$]	0.0732
$wR2$ [b] (all data)	0.2046
Largest diff. peak and hole [e.Å^{-3}]	0.50 and -0.64

a: $R1 = (\sum||F_o|-|F_c||)/(\sum|F_o|)$. b: $wR2 = [\sum w(F_o^2-F_c^2)^2/\sum wF_o^4]^{1/2}$, where $w = 1/[\sigma^2(F_o^2)+(0.1000(F_o^2+2F_c^2)/3)^2+ 4.8600(F_o^2+2F_c^2)/3]$

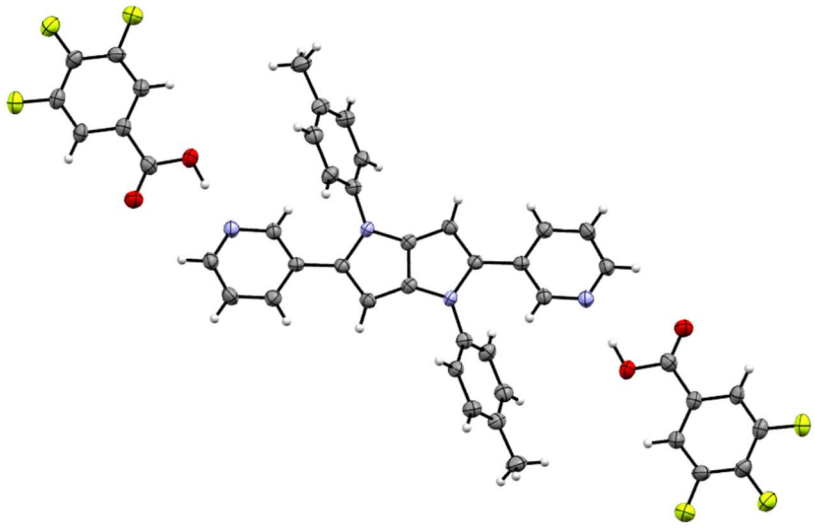

Fig. S10 Crystal structure of **1•e** (123 K). Ellipsoids are plotted at the 50% probability level.

Table S10 Crystallographic data for **1•e** (123 K).

Compound	**1•e**
CCDC No.	1910447
empirical formula	$C_{44}H_{30}F_6N_4O_4$
formula weight	792.72
temperature [K]	123
wavelength [Å]	0.71073
crystal system	monoclinic
space group	$P2_1/c$
a [Å]	5.9103(5)
b [Å]	18.358(2)
c [Å]	17.0558(19)
α [°]	90
β [°]	92.591(9)
γ [°]	90
Volume [Å^3]	1848.7(3)
Z	2
Density (calculated) [g/cm^3]	1.424
Absorption coefficient [mm^{-1}]	0.113
F(000)	816.0
θ [°]	2.52 to 26.371
Reflections collected	11892
Independent reflections	3775 [$R_{(int)}$ = 0.1341]
Data / restraints / parameters	3775 / 0 / 267
Goodness-of-fit on F^2	1.007
$R1$[a] [$I>2\sigma(I)$]	0.0732
$wR2$ [b] (all data)	0.2228
Largest diff. peak and hole [e.Å^{-3}]	0.36 and -0.34

a: $R1= (\sum||F_o|-|F_c||)/(\sum|F_o|)$. b: $wR2= [\sum w(F_o^2-F_c^2)^2/\sum wF_o^4]^{1/2}$, where $w= 1/[\sigma^2(F_o^2)+(0.0640(F_o^2+2F_c^2)/3)^2]$

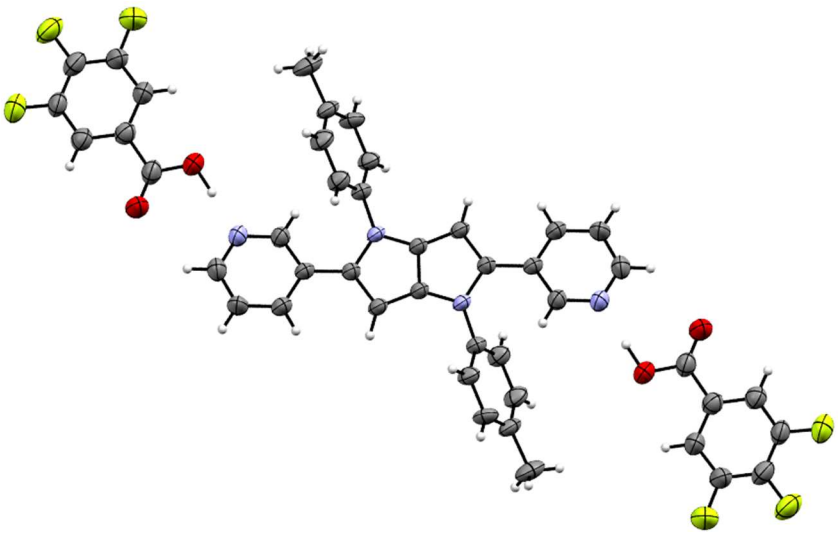

Fig. S11 Crystal structure of **1•e** (298 K). Ellipsoids are plotted at the 50% probability level.

Table S11 Crystallographic data for **1•e** (298 K).

Compound	**1•e**
CCDC No.	1910448
empirical formula	$C_{44}H_{30}F_6N_4O_4$
formula weight	792.72
temperature [K]	298
wavelength [Å]	0.71073
crystal system	monoclinic
space group	$P2_1/c$
a [Å]	5.8781(5)
b [Å]	18.3134(19)
c [Å]	17.3997(18)
α [°]	90
β [°]	93.672(9)
γ [°]	90
Volume [Å^3]	1869.2(3)
Z	2
Density (calculated) [g/cm^3]	1.408
Absorption coefficient [mm^{-1}]	0.113
F(000)	816.0
θ [°]	2.515 to 26.37
Reflections collected	12241
Independent reflections	3822 [$R_{(int)}$ = 0.1341]
Data / restraints / parameters	3822 / 0 / 267
Goodness-of-fit on F^2	0.992
$R1$[a] [$I>2\sigma(I)$]	0.0619
$wR2$[b] (all data)	0.1645
Largest diff. peak and hole [e.Å^{-3}]	0.17 and -0.25

a: $R1 = (\sum||F_o|-|F_c||)/(\sum|F_o|)$. b: $wR2 = [\sum w(F_o^2-F_c^2)^2/\sum wF_o^4]^{1/2}$, where $w = 1/[\sigma^2(F_o^2)+(0.0350(F_o^2+2F_c^2)/3)^2]$

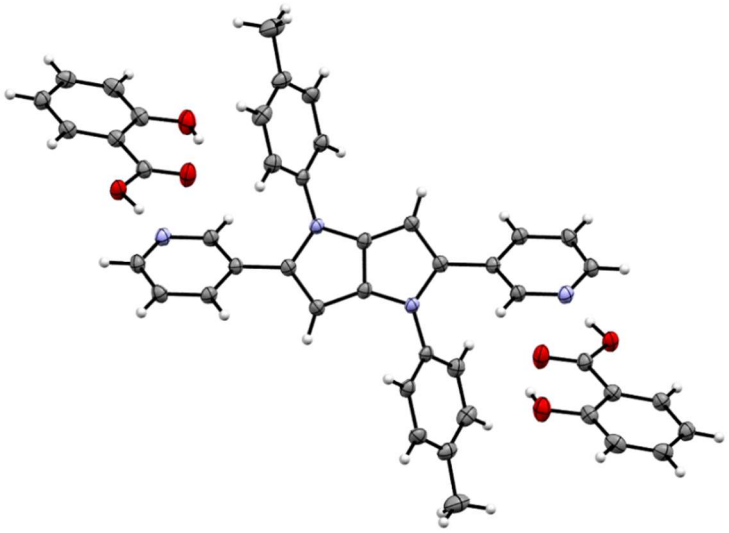

Fig. S12 Crystal structure of **1•f** (123 K). Ellipsoids are plotted at the 50% probability level.

Table S12 Crystallographic data for **1•f** (123 K**).**

Compound	**1•f**
CCDC No.	1910450
empirical formula	$C_{44}H_{36}N_4O_6$
formula weight	716.77
temperature [K]	123
wavelength [Å]	0.71073
crystal system	triclinic
space group	P -1
a [Å]	6.5494(3)
b [Å]	12.4521(7)
c [Å]	12.9443(8)
α [°]	112.739(6)
β [°]	101.751(5)
γ [°]	102.668(4)
Volume [Å^3]	899.78(10)
Z	1
Density (calculated) [g/cm^3]	1.323
Absorption coefficient [mm^{-1}]	0.089
F(000)	376.0
θ [°]	3.136 to 26.37
Reflections collected	7850
Independent reflections	3668 [$R_{(int)}$ = 0.0252]
Data / restraints / parameters	3668 / 0 / 250
Goodness-of-fit on F^2	1.023
$R1$[a] [$I>2\sigma(I)$]	0.0404
$wR2$ [b] (all data)	0.1186
Largest diff. peak and hole [e.Å^{-3}]	0.28 and -0.21

a: $R1= (\sum||F_o|-|F_c||)/(\sum|F_o|)$. b: $wR2= [\sum w(F_o^2-F_c^2)^2/\sum wF_o^4]^{1/2}$, where $w= 1/[\sigma^2(F_o^2)+(0.0590(F_o^2+2F_c^2)/3)^2+ 0.3020(F_o^2+2F_c^2)/3]$

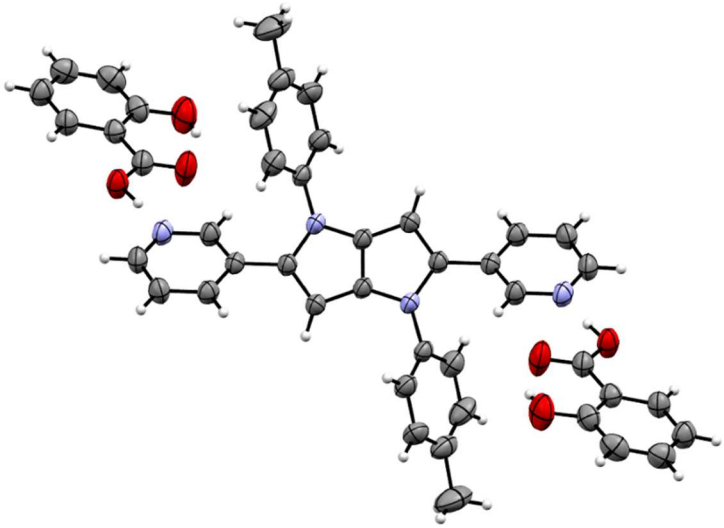

Fig. S13 Crystal structure of **1•f** (298 K). Ellipsoids are plotted at the 50% probability level.

Table S13 Crystallographic data for **1•f** (298 K).

Compound	**1•f**
CCDC No.	1910449
empirical formula	$C_{44}H_{36}N_4O_6$
formula weight	716.77
temperature [K]	298
wavelength [Å]	0.71073
crystal system	triclinic
space group	P -1
a [Å]	6.5951(7)
b [Å]	12.5932(13)
c [Å]	13.1549(16)
α [°]	116.795(11)
β [°]	95.657(9)
γ [°]	102.311(9)
Volume [Å^3]	928.8(2)
Z	1
Density (calculated) [g/cm^3]	1.281
Absorption coefficient [mm^{-1}]	0.086
F(000)	376.0
θ [°]	3.117 to 26.371
Reflections collected	7632
Independent reflections	3789 [$R_{(int)}$ = 0.0200]
Data / restraints / parameters	3789 / 0 / 250
Goodness-of-fit on F^2	1.010
$R1$[a] [$I>2\sigma(I)$]	0.0424
$wR2$ [b] (all data)	0.1346
Largest diff. peak and hole [e.Å^{-3}]	0.15 and -0.16

a: $R1= (\sum||F_o|-|F_c||)/(\sum|F_o|)$. b: $wR2= [\sum w(F_o^2-F_c^2)^2/\sum wF_o^4]^{1/2}$, where $w= 1/[\sigma^2(F_o^2)+(0.0710(F_o^2+2F_c^2)/3)^2+ 0.1390(F_o^2+2F_c^2)/3]$

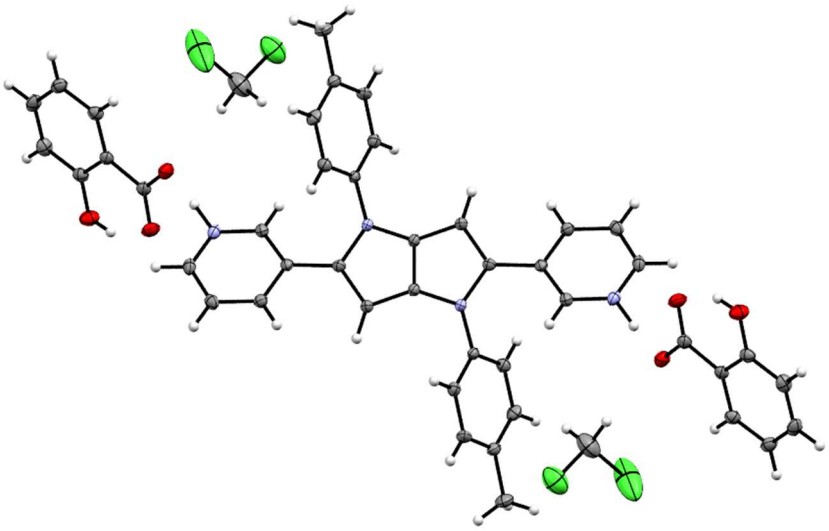

Fig. S14 Crystal structure of **1•f**⊃CH_2Cl_2 (123 K). Ellipsoids are plotted at the 50% probability level.

Table S14 Crystallographic data for **1•f**⊃CH_2Cl_2 (123 K).

Compound	**1•f**⊃CH_2Cl_2
CCDC No.	1910452
empirical formula	$C_{46}H_{40}Cl_4N_4O_6$
formula weight	886.62
temperature [K]	123
wavelength [Å]	0.71073
crystal system	triclinic
space group	P -1
a [Å]	9.5466(5)
b [Å]	10.9106(5)
c [Å]	11.4827(5)
α [°]	75.419(4)
β [°]	67.639(5)
γ [°]	84.290(4)
Volume [Å^3]	1070.46(10)
Z	1
Density (calculated) [g/cm^3]	1.375
Absorption coefficient [mm^{-1}]	0.331
F(000)	460.0
θ [°]	2.787 to 26.372
Reflections collected	9253
Independent reflections	4372 [$R_{(int)}$ = 0.0132]
Data / restraints / parameters	4372 / 0 / 277
Goodness-of-fit on F^2	1.048
$R1$[a] [$I>2\sigma(I)$]	0.0406
$wR2$ [b] (all data)	0.1088
Largest diff. peak and hole [e.Å^{-3}]	0.46 and -0.66

a: $R1 = (\sum||F_o|-|F_c||)/(\sum|F_o|)$. b: $wR2 = [\sum w(F_o^2-F_c^2)^2/\sum wF_o^4]^{1/2}$, where $w = 1/[\sigma^2(F_o^2)+(0.0510(F_o^2+2F_c^2)/3)^2+ 0.7050(F_o^2+2F_c^2)/3]$

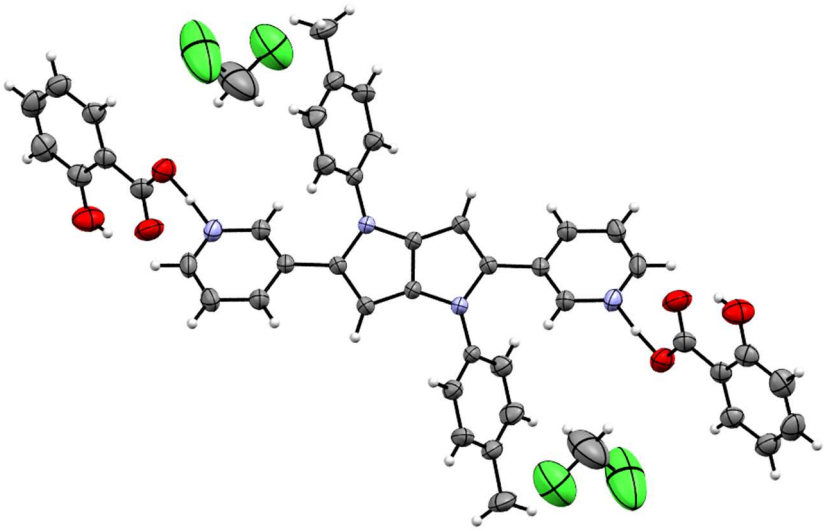

Fig. S15 Crystal structure of **1•f**⊃CH_2Cl_2 (298 K). Ellipsoids are plotted at the 50% probability level.

Table S15 Crystallographic data for **1•f**⊃CH_2Cl_2 (298 K).

Compound	**1•f**⊃CH_2Cl_2
CCDC No.	1910451
empirical formula	$C_{46}H_{40}Cl_4N_4O_6$
formula weight	886.62
temperature [K]	298
wavelength [Å]	0.71073
crystal system	triclinic
space group	P -1
a [Å]	9.5614(7)
b [Å]	10.9763(9)
c [Å]	11.7461(7)
α [°]	75.295(6)
β [°]	67.456(6)
γ [°]	84.613(7)
Volume [Å^3]	1101.24(15)
Z	1
Density (calculated) [g/cm^3]	1.337
Absorption coefficient [mm^{-1}]	0.321
F(000)	460.0
θ [°]	2.772 to 26.372
Reflections collected	9736
Independent reflections	4501 [$R_{(int)}$ = 0.0166]
Data / restraints / parameters	4501 / 0 / 277
Goodness-of-fit on F^2	1.050
$R1$[a] [$I>2\sigma(I)$]	0.0588
$wR2$ [b] (all data)	0.1881
Largest diff. peak and hole [e.Å^{-3}]	0.52 and -0.62

a: $R1= (\sum||F_o|-|F_c||)/(\sum|F_o|)$. b: $wR2= [\sum w(F_o^2-F_c^2)^2/\sum wF_o^4]^{1/2}$, where $w= 1/[\sigma^2(F_o^2)+(0.0980(F_o^2+2F_c^2)/3)^2+ 0.5430(F_o^2+2F_c^2)/3]$

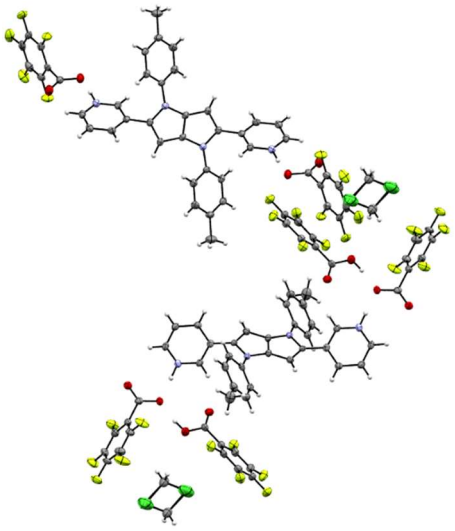

Fig. S16 Crystal structure of **1•g**⊃CH_2Cl_2 (123 K). Ellipsoids are plotted at the 50% probability level.

Table S16 Crystallographic data for **1•g**⊃CH_2Cl_2 (123 K).

Compound	**1•g**⊃CH_2Cl_2
CCDC No.	1910453
empirical formula	$C_{103}H_{56}Cl_2F_{30}N_8O_{12}$
formula weight	2238.45
temperature [K]	123
wavelength [Å]	0.71073
crystal system	triclinic
space group	P -1
a [Å]	13.6508(15)
b [Å]	13.6780(10)
c [Å]	13.7140(13)
α [°]	116.795(11)
β [°]	74.923(9)
γ [°]	71.683(8)
Volume [Å^3]	2336.1(4)
Z	1
Density (calculated) [g/cm^3]	1.591
Absorption coefficient [mm^{-1}]	0.200
F(000)	1130.0
θ [°]	2.467 to 26.372
Reflections collected	21230
Independent reflections	9521 [$R_{(int)}$ = 0.0626]
Data / restraints / parameters	9521 / 0 / 726
Goodness-of-fit on F^2	1.062
$R1$[a] [$I>2\sigma(I)$]	0.0630
$wR2$ [b] (all data)	0.2146
Largest diff. peak and hole [e.Å^{-3}]	0.33 and -0.34

a: $R1 = (\sum||F_o|-|F_c||)/(\sum|F_o|)$. b: $wR2 = [\sum w(F_o^2-F_c^2)^2/\sum wF_o^4]^{1/2}$, where $w = 1/[\sigma^2(F_o^2)+(0.1000(F_o^2+2F_c^2)/3)^2]$

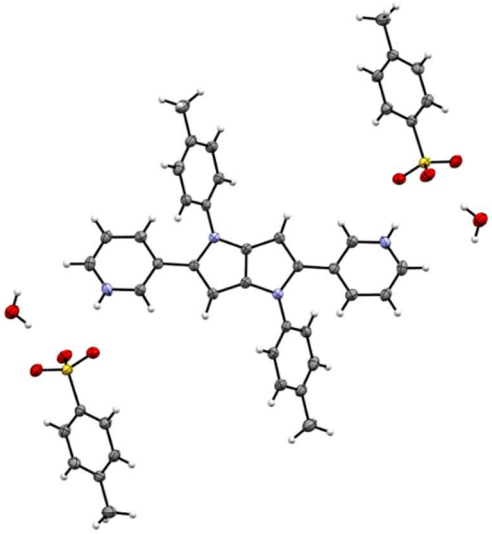

Fig. S17 Crystal structure of **1•h**⊃H_2O (123 K). Ellipsoids are plotted at the 50% probability level.

Table S17 Crystallographic data for **1•h**⊃H_2O (123 K).

Compound	**1•h**⊃H_2O
CCDC No.	1910454
empirical formula	$C_{44}H_{44}N_4O_8S_2$
formula weight	820.95
temperature [K]	123
wavelength [Å]	0.71073
crystal system	triclinic
space group	P -1
a [Å]	7.6993(4)
b [Å]	11.1583(9)
c [Å]	11.5390(10)
α [°]	89.783(7)
β [°]	85.718(6)
γ [°]	84.804(5)
Volume [Å^3]	984.49(13)
Z	1
Density (calculated) [g/cm^3]	1.385
Absorption coefficient [mm^{-1}]	0.197
F(000)	432.0
θ [°]	2.544 to 26.371
Reflections collected	8832
Independent reflections	4029 [$R_{(int)}$ = 0.0376]
Data / restraints / parameters	4029 / 0 / 271
Goodness-of-fit on F^2	1.085
$R1$[a] [$I>2\sigma(I)$]	0.0543
$wR2$ [b] (all data)	0.1547
Largest diff. peak and hole [e.Å^{-3}]	0.34 and -0.46

a: $R1 = (\sum||F_o|-|F_c||)/(\sum|F_o|)$. b: $wR2 = [\sum w(F_o^2-F_c^2)^2/\sum wF_o^4]^{1/2}$, where $w = 1/[\sigma^2(F_o^2)+(0.0650(F_o^2+2F_c^2)/3)^2+ 0.7200(F_o^2+2F_c^2)/3]$

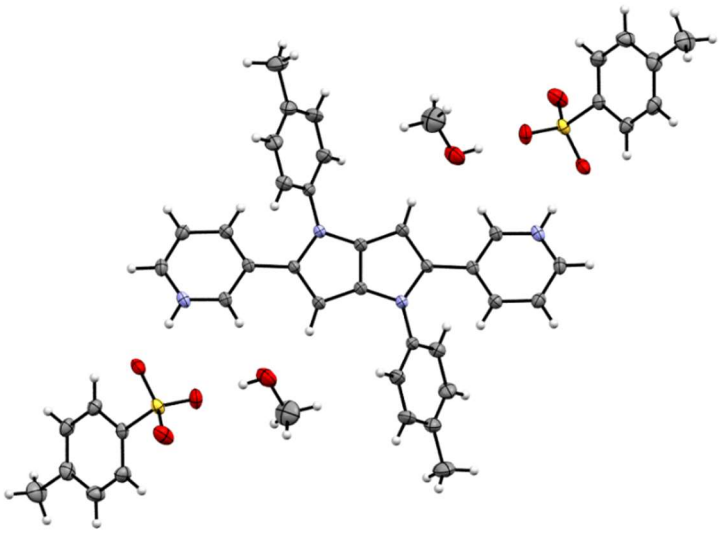

Fig. S18 Crystal structure of **1•h**⊃CH_3OH (123 K). Ellipsoids are plotted at the 50% probability level.

Table S18 Crystallographic data for **1•h**⊃CH_3OH (123 K).

Compound	**1•h**⊃CH_3OH
CCDC No.	1910455
empirical formula	$C_{46}H_{48}N_4O_8S_2$
formula weight	849.00
temperature [K]	123
wavelength [Å]	0.71073
crystal system	monoclinic
space group	$P2_1/n$
a [Å]	16.4360(4)
b [Å]	7.74190(10)
c [Å]	16.8951(4)
α [°]	90
β [°]	98.106(2)
γ [°]	90
Volume [Å^3]	2128.35(8)
Z	2
Density (calculated) [g/cm^3]	1.325
Absorption coefficient [mm^{-1}]	0.184
F(000)	896.0
θ [°]	2.899 to 26.37
Reflections collected	25342
Independent reflections	4353 [$R_{(int)}$ = 0.0254]
Data / restraints / parameters	4353 / 0 / 279
Goodness-of-fit on F^2	0.913
$R1$[a] [$I>2\sigma(I)$]	0.0381
$wR2$ [b] (all data)	0.1184
Largest diff. peak and hole [e.Å^{-3}]	0.34 and -0.36

a: $R1 = (\sum||F_o|-|F_c||)/(\sum|F_o|)$. b: $wR2 = [\sum w(F_o^2-F_c^2)^2/\sum wF_o^4]^{1/2}$, where $w = 1/[\sigma^2(F_o^2)+(0.0770(F_o^2+2F_c^2)/3)^2+ 1.6640(F_o^2+2F_c^2)/3]$

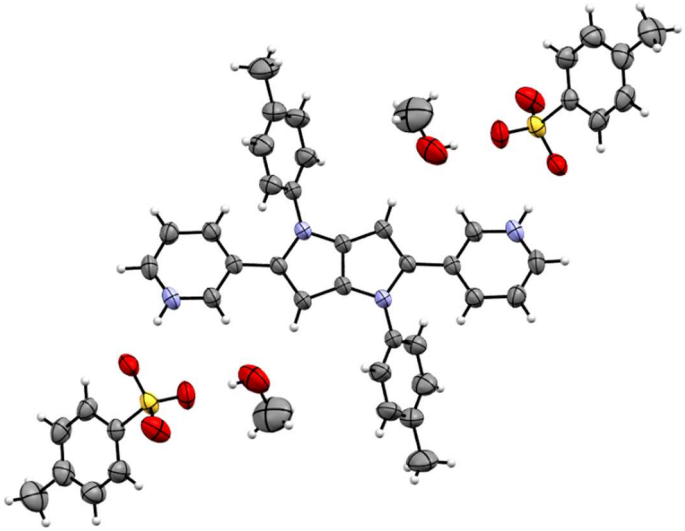

Fig. S19 Crystal structure of **1•h**⊃CH_3OH (298 K). Ellipsoids are plotted at the 50% probability level.

Table S19 Crystallographic data for **1•h**⊃CH_3OH (298 K).

Compound	**1•h**⊃CH_3OH
CCDC No.	1910456
empirical formula	$C_{46}H_{48}N_4O_8S_2$
formula weight	849.00
temperature [K]	298
wavelength [Å]	0.71073
crystal system	monoclinic
space group	$P2_1/n$
a [Å]	16.5791(7)
b [Å]	7.7313(3)
c [Å]	17.2465(8)
α [°]	90
β [°]	99.073(4)
γ [°]	90
Volume [Å^3]	2182.96(16)
Z	2
Density (calculated) [g/cm^3]	1.292
Absorption coefficient [mm^{-1}]	0.180
F(000)	896.0
θ [°]	2.893 to 26.367
Reflections collected	14532
Independent reflections	4466 [$R_{(int)}$ = 0.0197]
Data / restraints / parameters	4466 / 0 / 279
Goodness-of-fit on F^2	1.045
$R1$[a] [$I>2\sigma(I)$]	0.0434
$wR2$ [b] (all data)	0.1314
Largest diff. peak and hole [e.Å^{-3}]	0.21 and -0.29

a: $R1= (\sum||F_o|-|F_c||)/(\sum|F_o|)$. b: $wR2= [\sum w(F_o^2-F_c^2)^2/\sum wF_o^4]^{1/2}$, where $w= 1/[\sigma^2(F_o^2)+(0.0620(F_o^2+2F_c^2)/3)^2+ 0.7800(F_o^2+2F_c^2)/3]$

Table S20 Elemental analysis of **1**.

Compound	Observed			Calcd		
	C	H	N	C	H	N
1	81.40	5.51	12.73	81.79	5.49	12.72

Table S21 The pK_a of **a**-**h** and ΔpK_a (pK_a (**1**) [a]- pK_a (acid)).

	a	**b**	**c**	**d**	**e**	**f**	**g**	**h**
pK_a	10.0	8.2	5.5	4.2	3.5	2.9	1.5	-1.3
ΔpK_a	-4.3	-2.5	0.2	1.5	2.2	2.8	4.2	7.0

[a]The pK_a value of pyridyl moiety of **1** is assumed to 5.7, which is taken from the pK_a value of 3-methylpyridine.

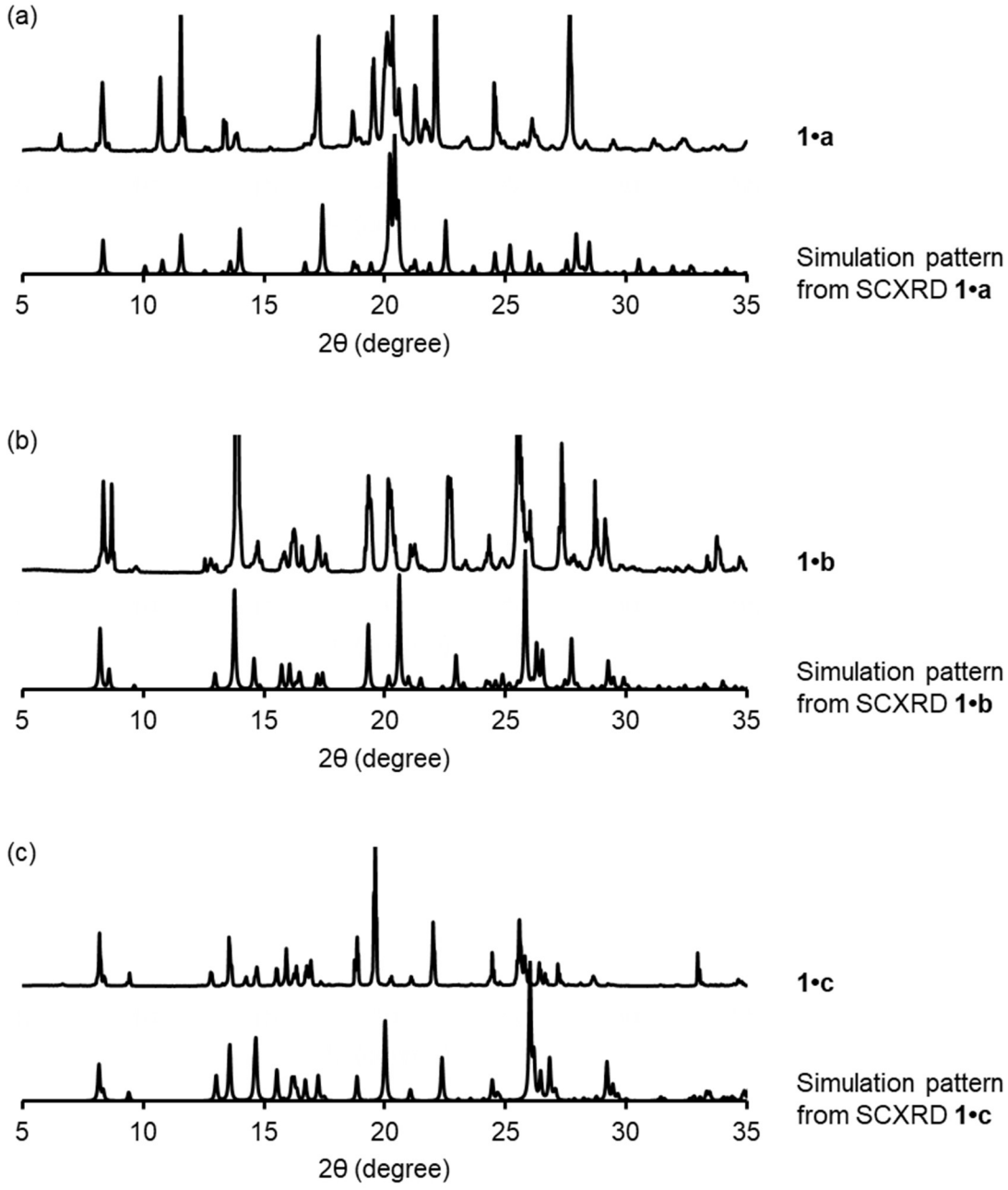
(a)
1•a
Simulation pattern from SCXRD 1•a
5
10
15
20
25
30
35
2θ (degree)
(b)
1•b
Simulation pattern from SCXRD 1•b
5
10
15
20
25
30
35
2θ (degree)
(c)
1•c
Simulation pattern from SCXRD 1•c
5
10
15
20
25
30
35
2θ (degree)

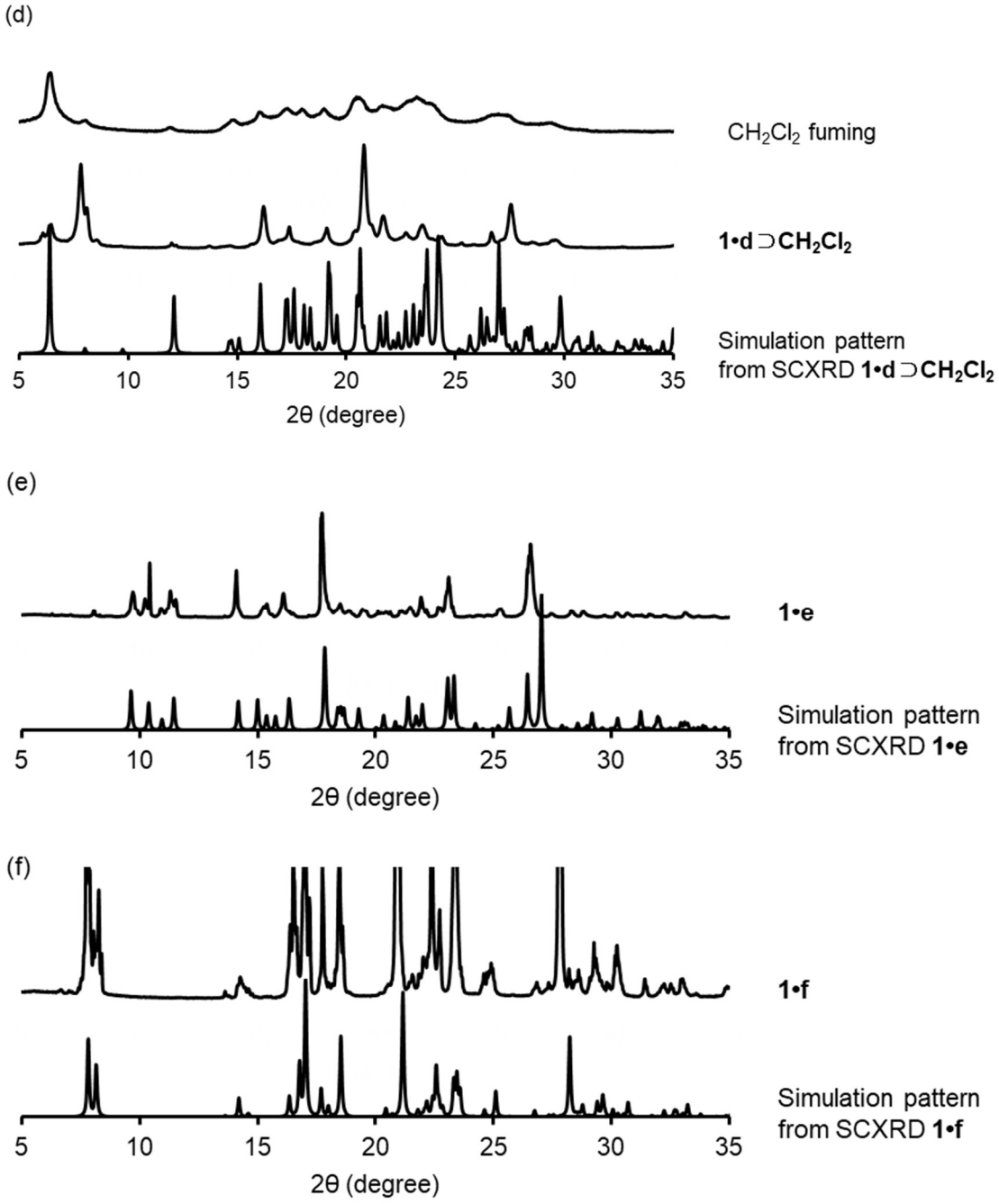
(d)
CH_2Cl_2 fuming
1•d⊃CH_2Cl_2
Simulation pattern
from SCXRD **1•d⊃CH_2Cl_2**
5
10
15
20
25
30
35
2θ (degree)
(e)
1•e
Simulation pattern
from SCXRD **1•e**
5
10
15
20
25
30
35
2θ (degree)
(f)
1•f
Simulation pattern
from SCXRD **1•f**
5
10
15
20
25
30
35
2θ (degree)

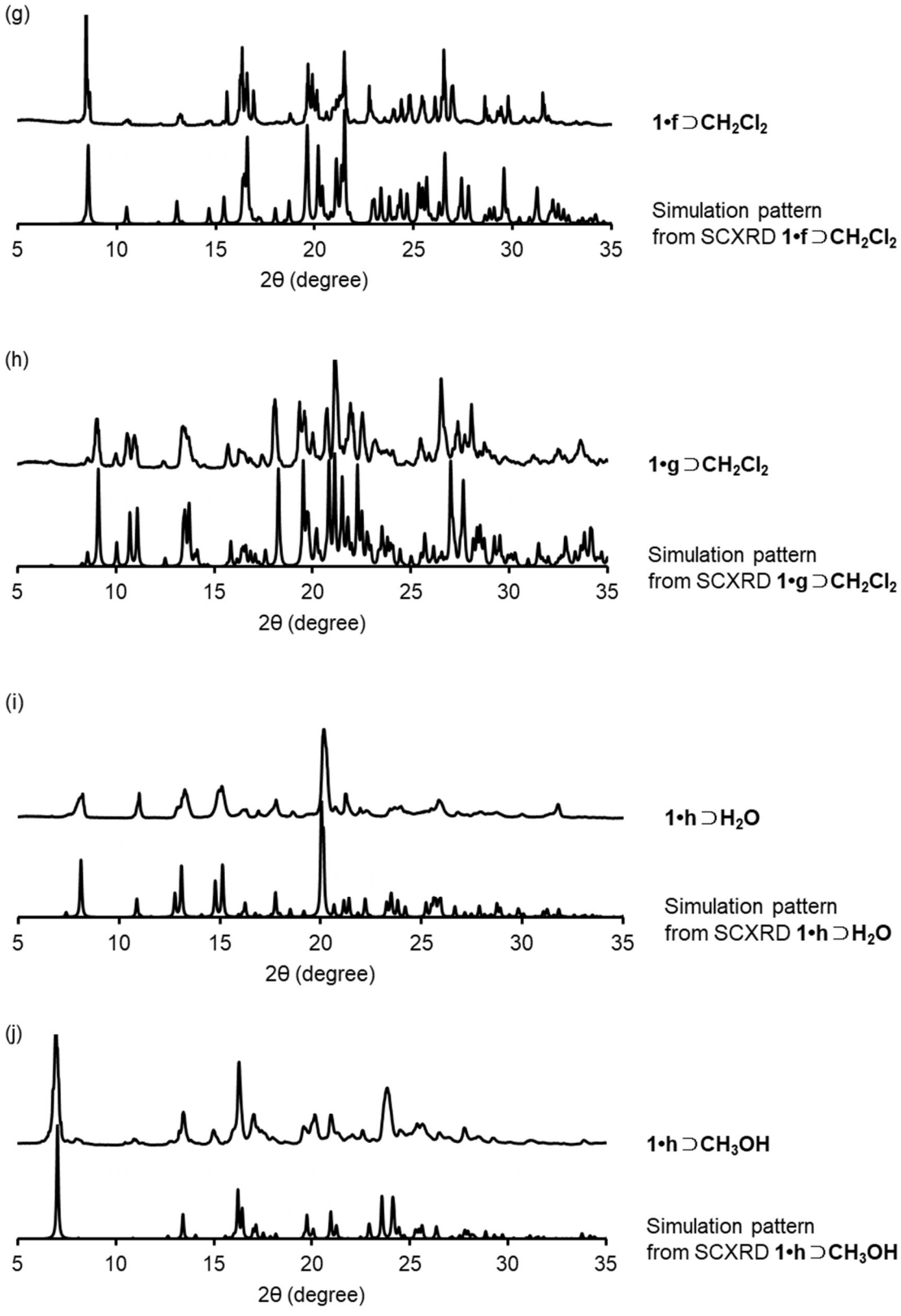
(g)
1•f⊃CH2Cl2
Simulation pattern from SCXRD 1•f⊃CH2Cl2
5 10 15 20 25 30 35
2θ (degree)
(h)
1•g⊃CH2Cl2
Simulation pattern from SCXRD 1•g⊃CH2Cl2
5 10 15 20 25 30 35
2θ (degree)
(i)
1•h⊃H2O
Simulation pattern from SCXRD 1•h⊃H2O
5 10 15 20 25 30 35
2θ (degree)
(j)
1•h⊃CH3OH
Simulation pattern from SCXRD 1•h⊃CH3OH
5 10 15 20 25 30 35
2θ (degree)

Fig. S20 PXRD patterns of **1•acid** (upper) and corresponding simulation pattern from SCXRD at 123K (lower) (a) **1•a**, (b) **1•b**, (c) **1•c**, (d) **1•d**⊃CH_2Cl_2, (e) **1•e**, (f) **1•f**, (g) **1•f**⊃CH_2Cl_2, (h) **1•g**⊃CH_2Cl_2, (i) **1•h**⊃H_2O, (j) **1•h**⊃CH_3OH. In the case of **1•d**⊃CH_2Cl_2, desorption of CH_2Cl_2 molecules is easily observed under room temperature. CH_2Cl_2 vapor exposure to the resulting complex regenerated the formation of **1•d**⊃CH_2Cl_2.

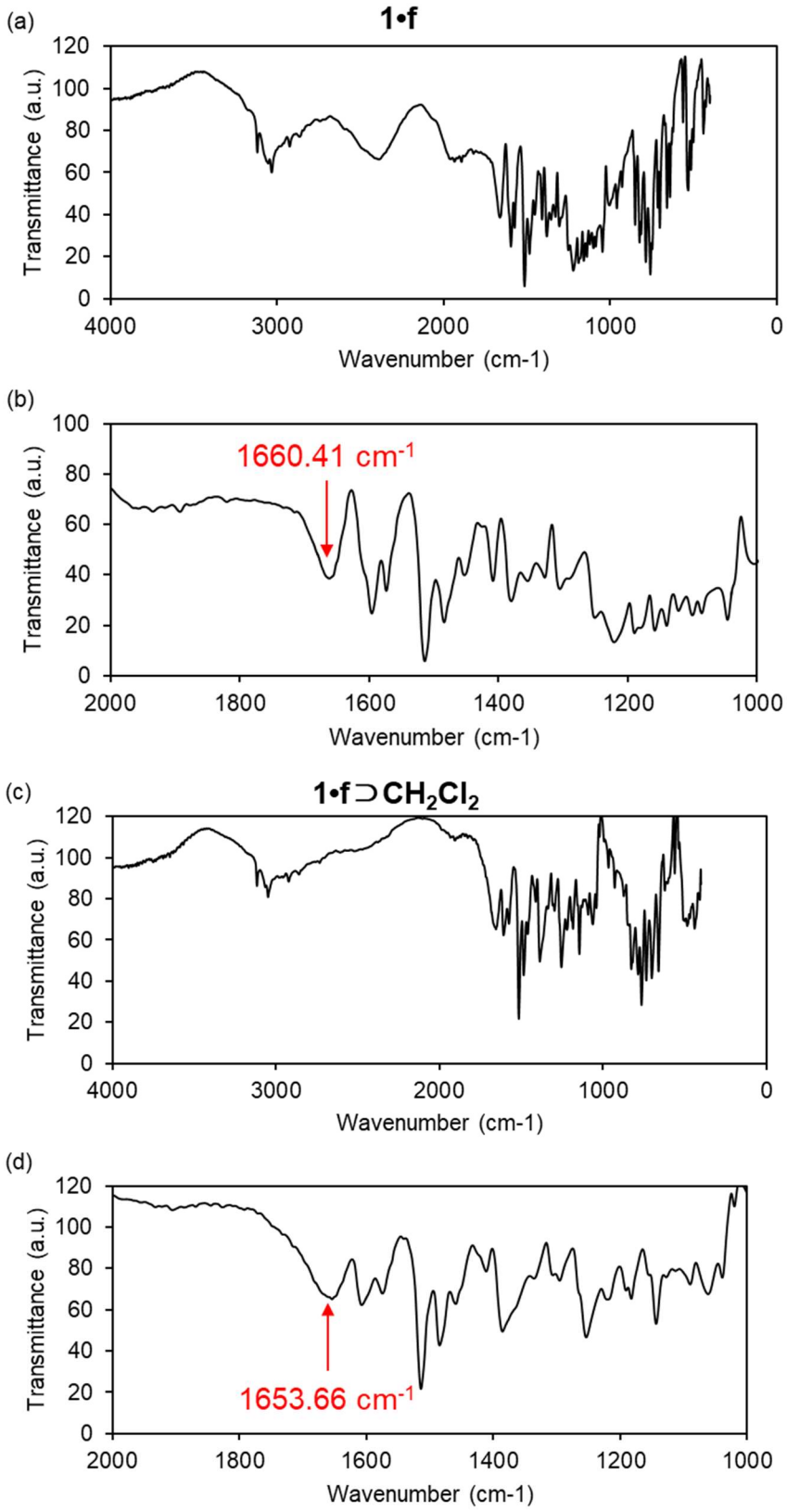

Fig. S21 IR spectra of **1•f** (a) 400-4000 cm^{-1}, (b) 1000-2000 cm^{-1}, and **1•f**⊃CH_2Cl_2 (c) 400-4000 cm^{-1}, (d) 1000-2000 cm^{-1}.

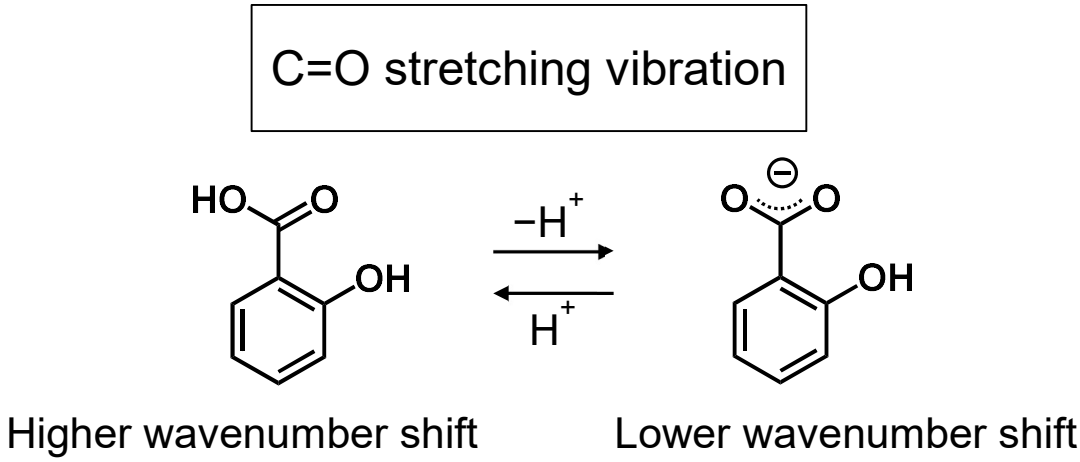

Scheme S1 Schematic illustration of protonation/deprotonation of salicylic acid estimated by IR spectra.

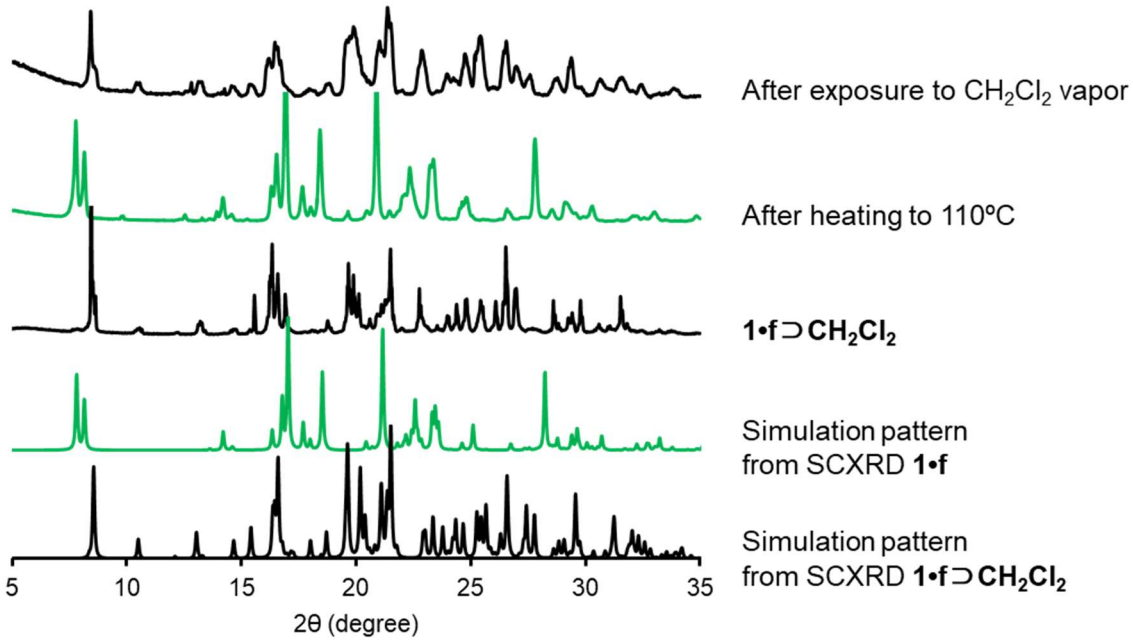

Fig. S22 PXRD patterns of **1•f**⊃CH_2Cl_2, after heating to 110ºC, and after exposure to CH_2Cl_2 vapor against resulting powder. Simulated patterns of **1•f**⊃CH_2Cl_2 and **1•f** from SCXRD are shown for comparison.

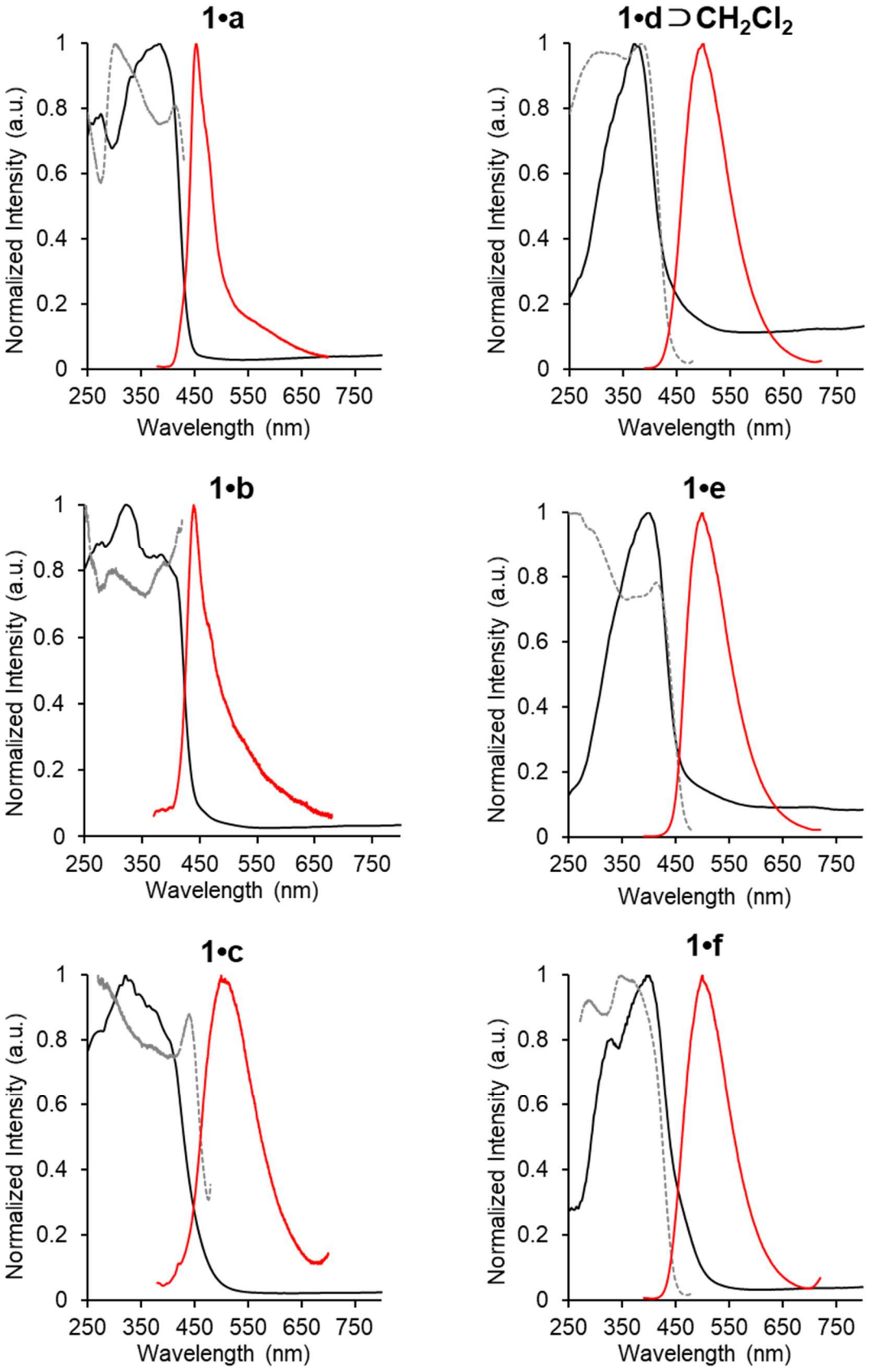
1•a
1•d⊃CH2Cl2
1•b
1•e
1•c
1•f
Normalized Intensity (a.u.)
Wavelength (nm)
0
0.2
0.4
0.6
0.8
1
250
350
450
550
650
750

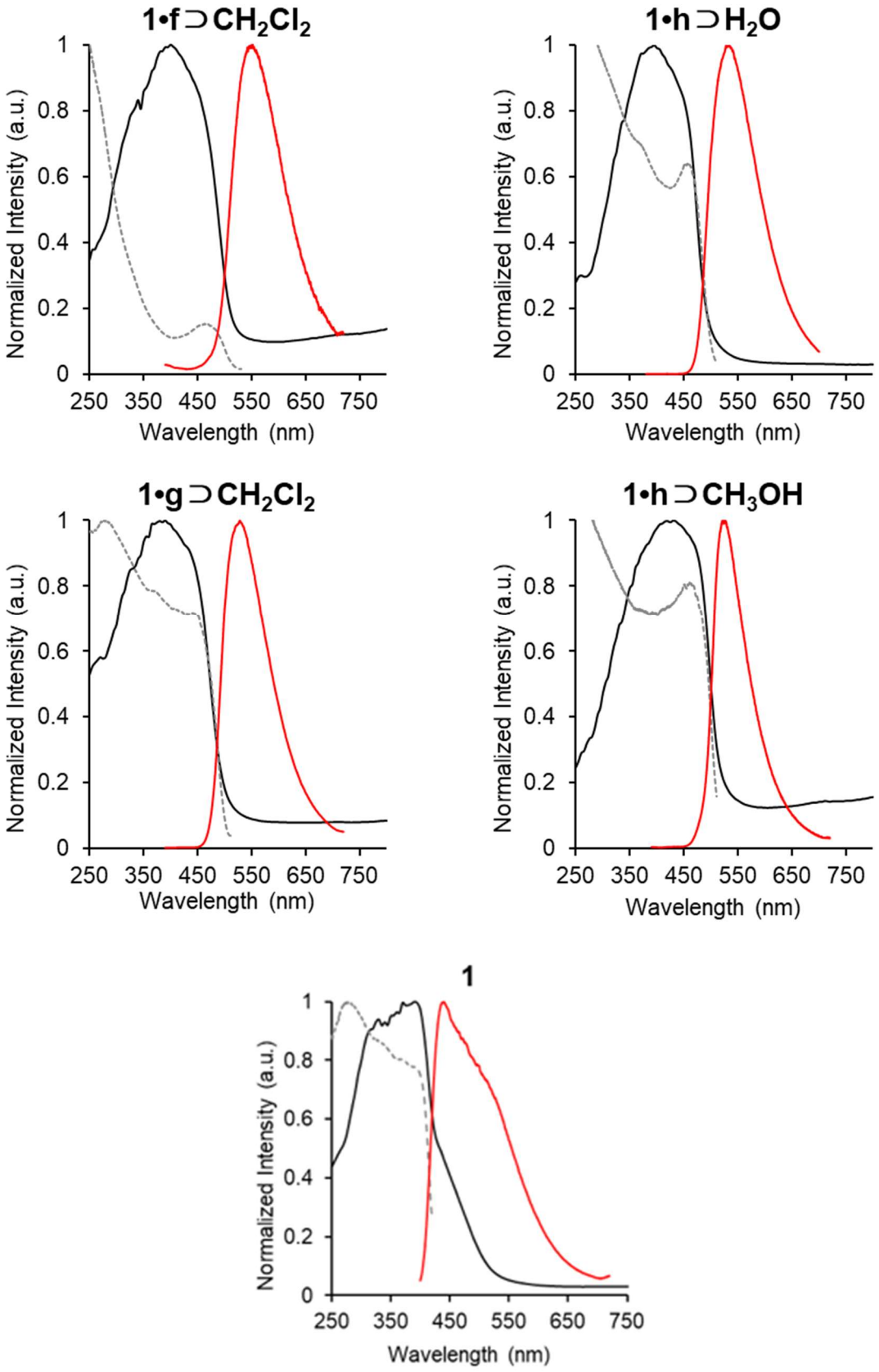

Fig. S23 UV-vis diffuse-reflectance spectra (black line), emission spectra (red line), and excitation spectra (dotted line) of **1** and **1•acid**.

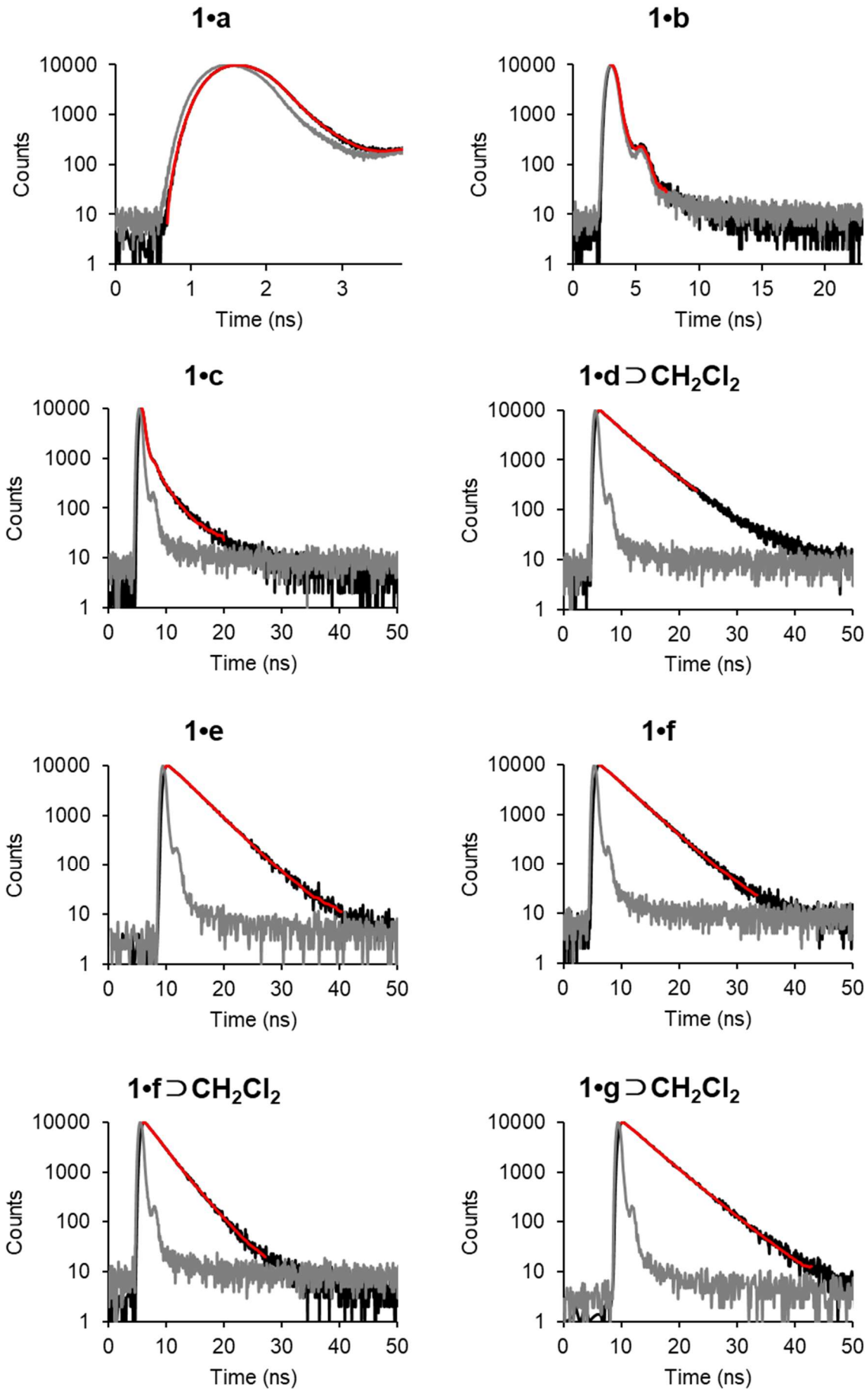
1•a
1•b
1•c
1•d⊃CH2Cl2
1•e
1•f
1•f⊃CH2Cl2
1•g⊃CH2Cl2
Counts
Time (ns)

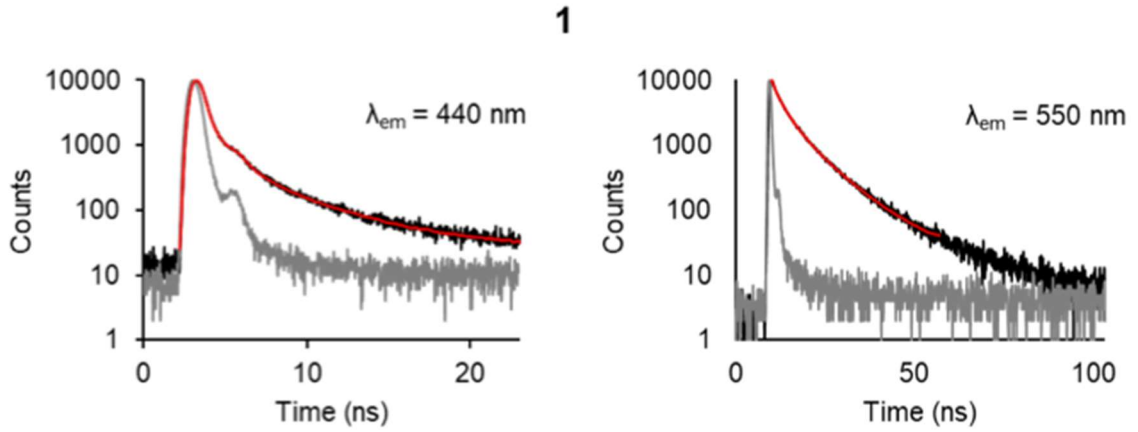

Fig. S24 Emission decay curves (black line), fits (red line), and instrument response function (IRF) of **1** and **1•acid**.

Table S22 Summary of lifetime analyses for **1** and **1•acid.** Emission lifetimes (τ), preexponetial factor in percentage (% A). λ = emission wavelength of registration after excitation at 365 nm and τ_{av} intensity average lifetime

sample	λ (nm)	CHI	τ_{av} (ns)	τ_1 (ns)	τ_2 (ns)	τ_3 (ns)	A_1	A_2	A_3
1	440	1.03	1.01	0.18	1.13	4.40	1134	64	12
1	550	1.08	5.9	0.8	3.2	8.9	676	630	307
1•a	453	1.02	0.1	0.1	0.5	-	336	2.3	-
1•b	439	1.17	0.1	0.08	0.21	0.68	1516	-135	3.4
1•c	500	1.19	0.9	0.3	2.3	-	2594	131	-
1•d⊃CH_2Cl_2	481	1.17	4.05	1.16	4.20	-	115	638	-
1•e	500	1.07	1.66	3.81	63.2	-	1380	-2.92	-
1•f	500	1.11	3.17	3.79	9.69	10.3	668	641	-572
1•f⊃CH_2Cl_2	552	1.02	2.35	2.48	6.73	7.42	686	474	-375
1•g⊃CH_2Cl_2	528	1.05	3.86	3.60	6.89	11.13	1026	451	-105
1•h⊃H_2O	534	1.10	1.93	0.73	2.15	-	628	1167	-
1•h⊃CH_3OH	524	1.03	3.05	1.12	3.3	-	435	1114	-

1

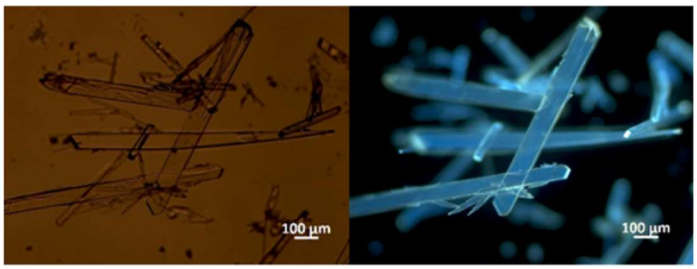

1•a

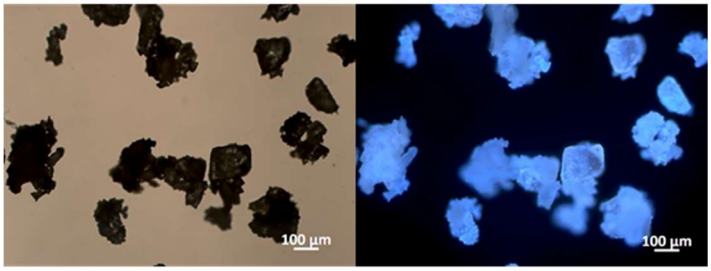

1•b

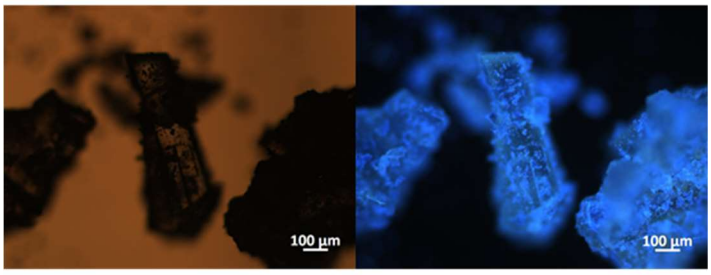

1•c

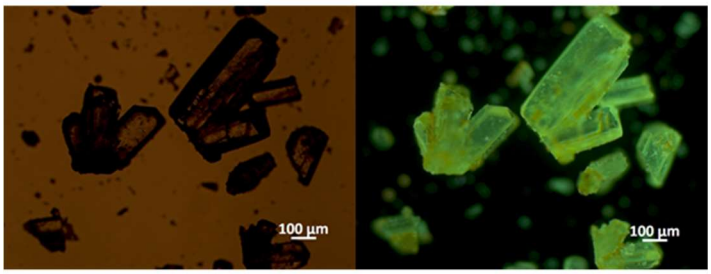

1•d ⊃ CH_2Cl_2

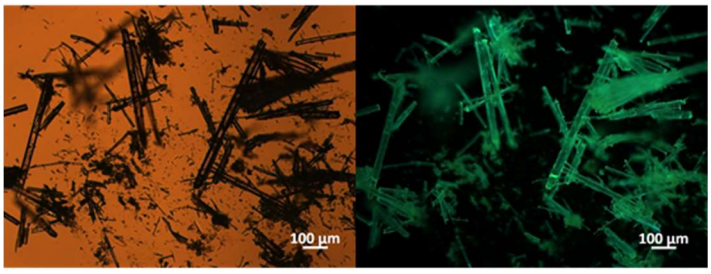

1•e

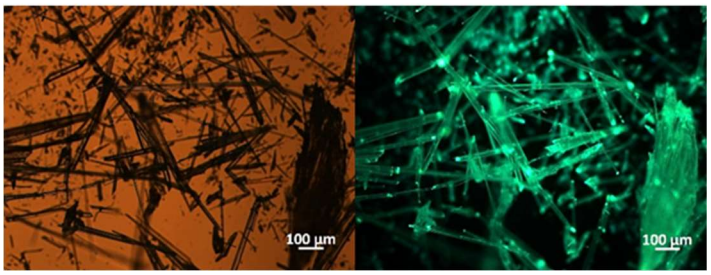

1•f

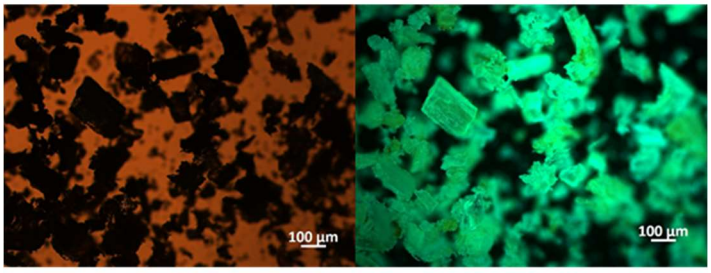

1•f⊃CH_2Cl_2

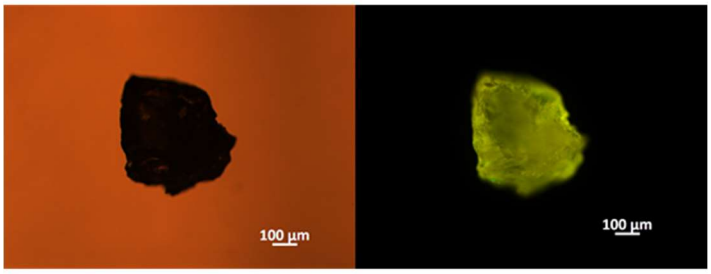

1•g⊃CH_2Cl_2

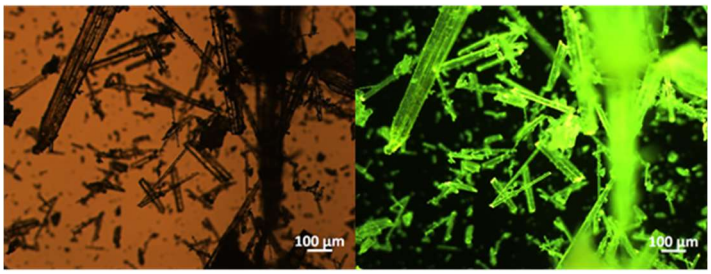

1•h⊃H_2O

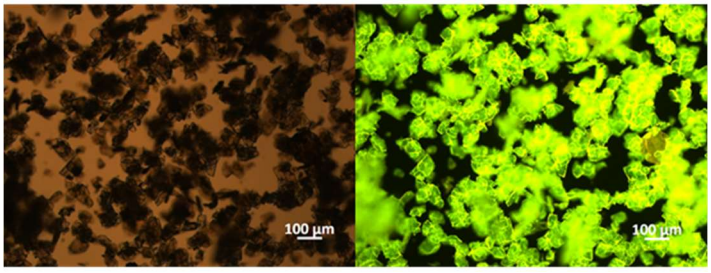

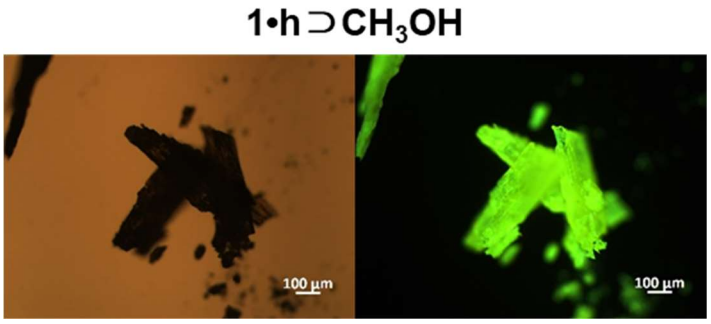

Fig. S25 Photographs of **1** and **1•acid** under fluorescence microscope. Excitation = 330-380 nm, Emission > 420 nm.

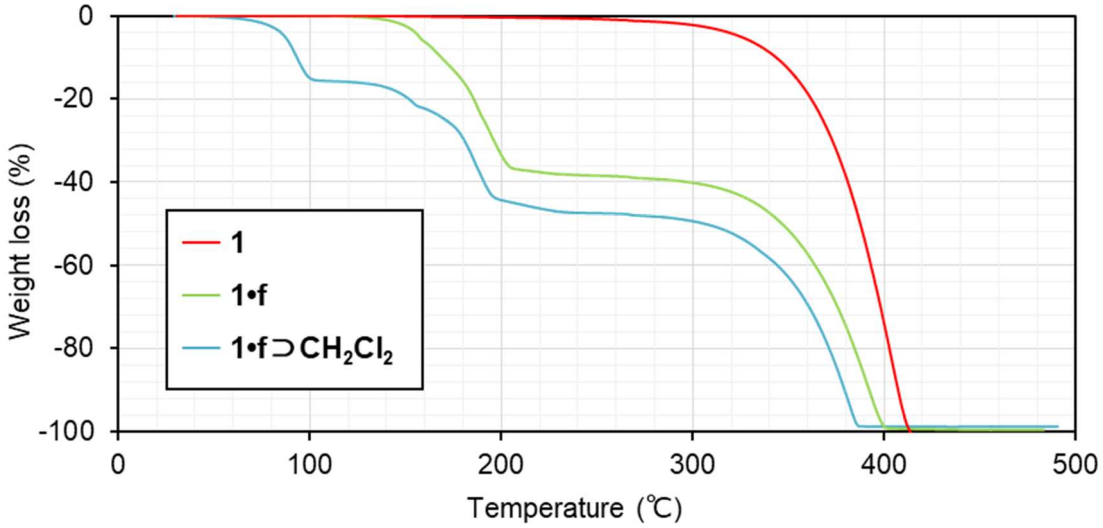

Fig. S26 TG analyzes of **1** (red line)**,** **1•f** (green line)**,** and **1•f**⊃CH_2Cl_2 (blue line)**.** The measurements were conducted in nitrogen atmosphere at a heating rate of 10ºC min^{-1}, and the weights of samples were normalized to 100%. The result indicated that guest (CH_2Cl_2) removal of **1•f**⊃CH_2Cl_2 is ca. 80ºC.

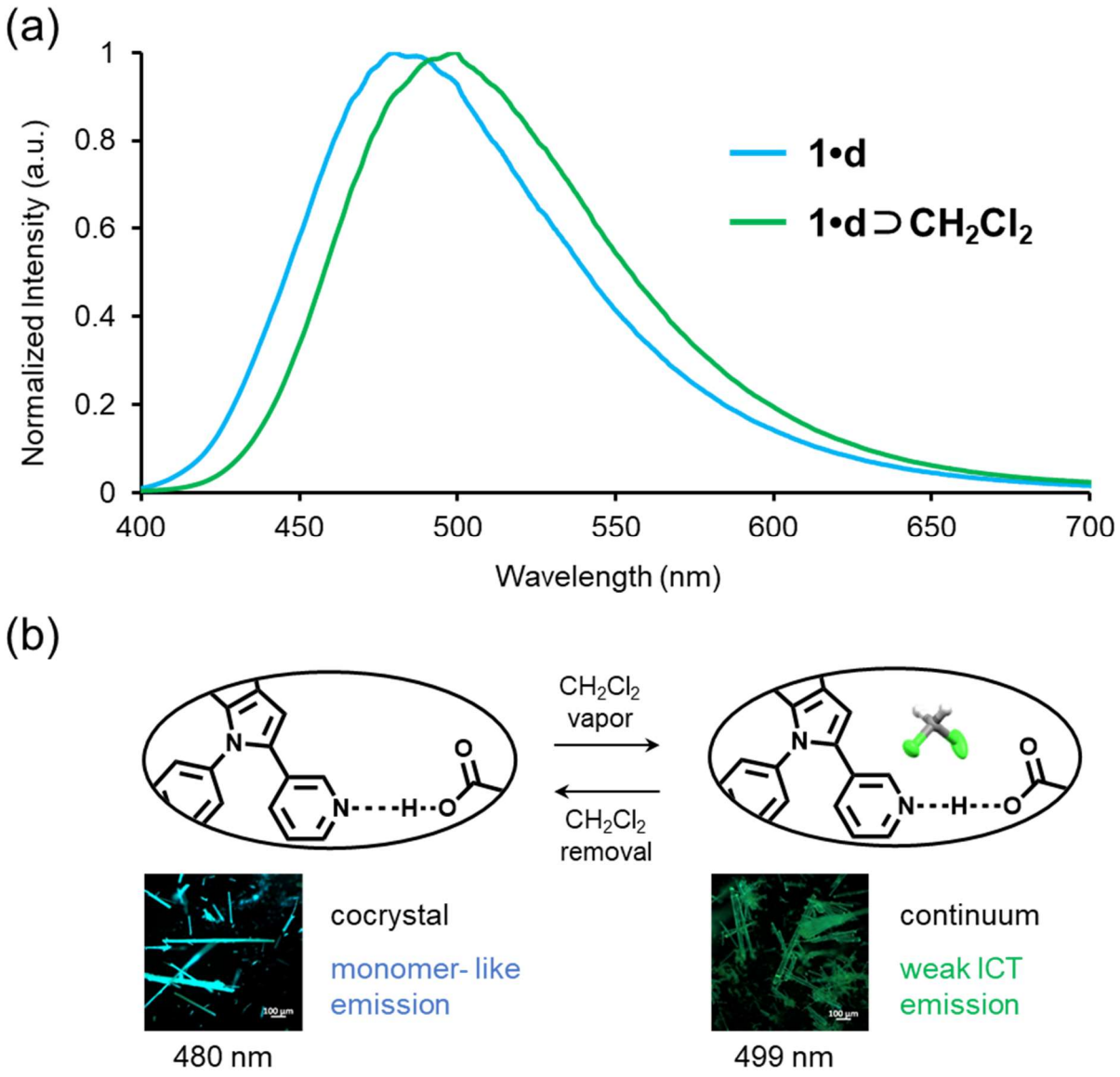

Fig. S27 (a) Emission spectra of **1•d** and **1•d**⊃CH_2Cl_2. Excitation at 370 nm. (b) Schematic illustration of emission color tuning depends on desorption and inclusion of CH_2Cl_2 against complexes.

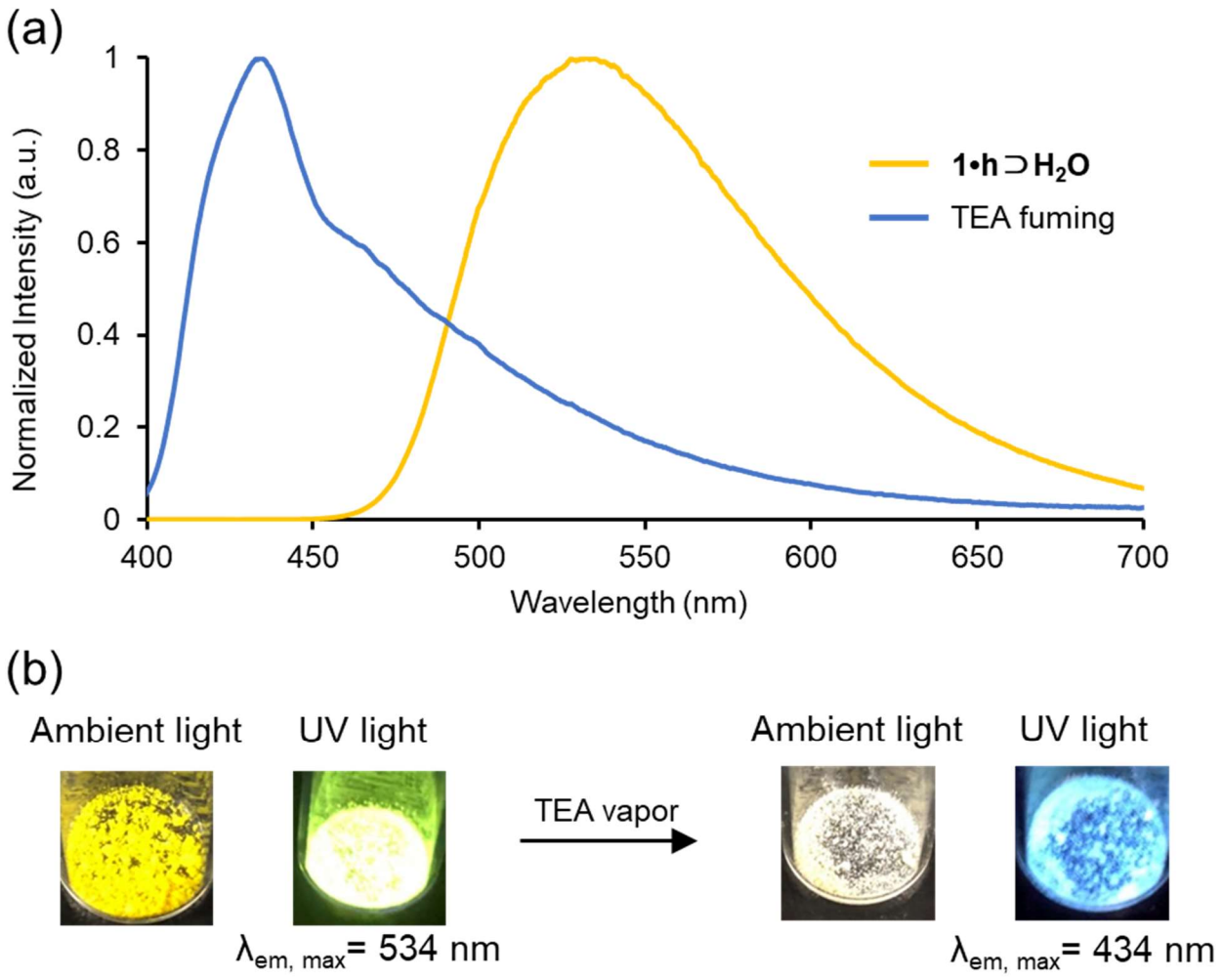

Fig. S28 (a) Emission spectra of **1•f**, and after fuming TEA vapor. (b) Photo of **1•f**, and after fuming TEA vapor.

General method of UV-Vis and fluorescence titration

1 and **f** in CH_2Cl_2 solution

Path length of the cells used for absorption and emission studies was 1cm. The stock solution of **1** was prepared (2.5×10^{-4} M) in CH_2Cl_2 (Stock A). The stock solution of acid (**f**) was prepared (2.5×10^{-4} M) in CH_2Cl_2 (Stock B). Stock A, Stock B, and CH_2Cl_2 were mixed according to Table S23, and UV-vis and emission spectra were measured. Final concentration of **1** is 2.5×10^{-5} M.

Table S23 Mixing condition of **1** and **f** in CH_2Cl_2.

Equivalent of **f** to **1**	Stock A	Stock B	CH_2Cl_2
0 eq.	500 μl	0 μl	4500 μl
1 eq.	500 μl	50 μl	4450 μl
2 eq.	500 μl	100 μl	4400 μl
3 eq.	500 μl	150 μl	4350 μl
4 eq.	500 μl	200 μl	4300 μl
5 eq.	500 μl	250 μl	4250 μl
6 eq.	500 μl	300 μl	4200 μl
7 eq.	500 μl	350 μl	4150 μl
8 eq.	500 μl	400 μl	4100 μl
9 eq.	500 μl	450 μl	4050 μl
10 eq.	500 μl	500 μl	4000 μl

1 and **g** in $CHCl_3$ solution

Path length of the cells used for absorption and emission studies was 1cm. The stock solutions of **1** was prepared (2.5×10^{-4} M) in $CHCl_3$ (Stock C). The stock solutions of acid (**g**) was prepared (2.5×10^{-4} M) in $CHCl_3$ (Stock D). Stock C, Stock D, and $CHCl_3$ were mixed according to Table S24, and UV-vis and emission spectra were measured. Final concentration of **1** is 2.5×10^{-5} M. $CHCl_3$ was used due to **g** was poor solubility in CH_2Cl_2.

Table S24 Mixing condition of **1** and **g** in $CHCl_3$.

Equivalent of **g** to **1**	Stock C	Stock D	CH_2Cl_2
0 eq.	500 µl	0 µl	4500 µl
0.5 eq.	500 µl	25 µl	4475 µl
1 eq.	500 µl	50 µl	4450 µl
1.5 eq.	500 µl	75 µl	4425 µl
2 eq.	500 µl	100 µl	4400 µl
2.5 eq.	500 µl	125 µl	4375 µl
3 eq.	500 µl	150 µl	4350 µl
3.5 eq.	500 µl	175 µl	4325 µl
4 eq.	500 µl	200 µl	4300 µl
4.5 eq.	500 µl	225 µl	4275 µl
5 eq.	500 µl	250 µl	4250 µl
5.5 eq.	500 µl	275 µl	4225 µl
6 eq.	500 µl	300 µl	4200 µl
6.5	500 µl	325 µl	4175 µl
7 eq.	500 µl	350 µl	4150 µl
7.5 eq.	500 µl	375 µl	4125 µl
8 eq.	500 µl	400 µl	4100 µl
8.5 eq.	500 µl	425 µl	4075 µl
9 eq.	500 µl	450 µl	4050 µl
9.5eq.	500 µl	475 µl	4025 µl
10 eq.	500 µl	500 µl	4000 µl

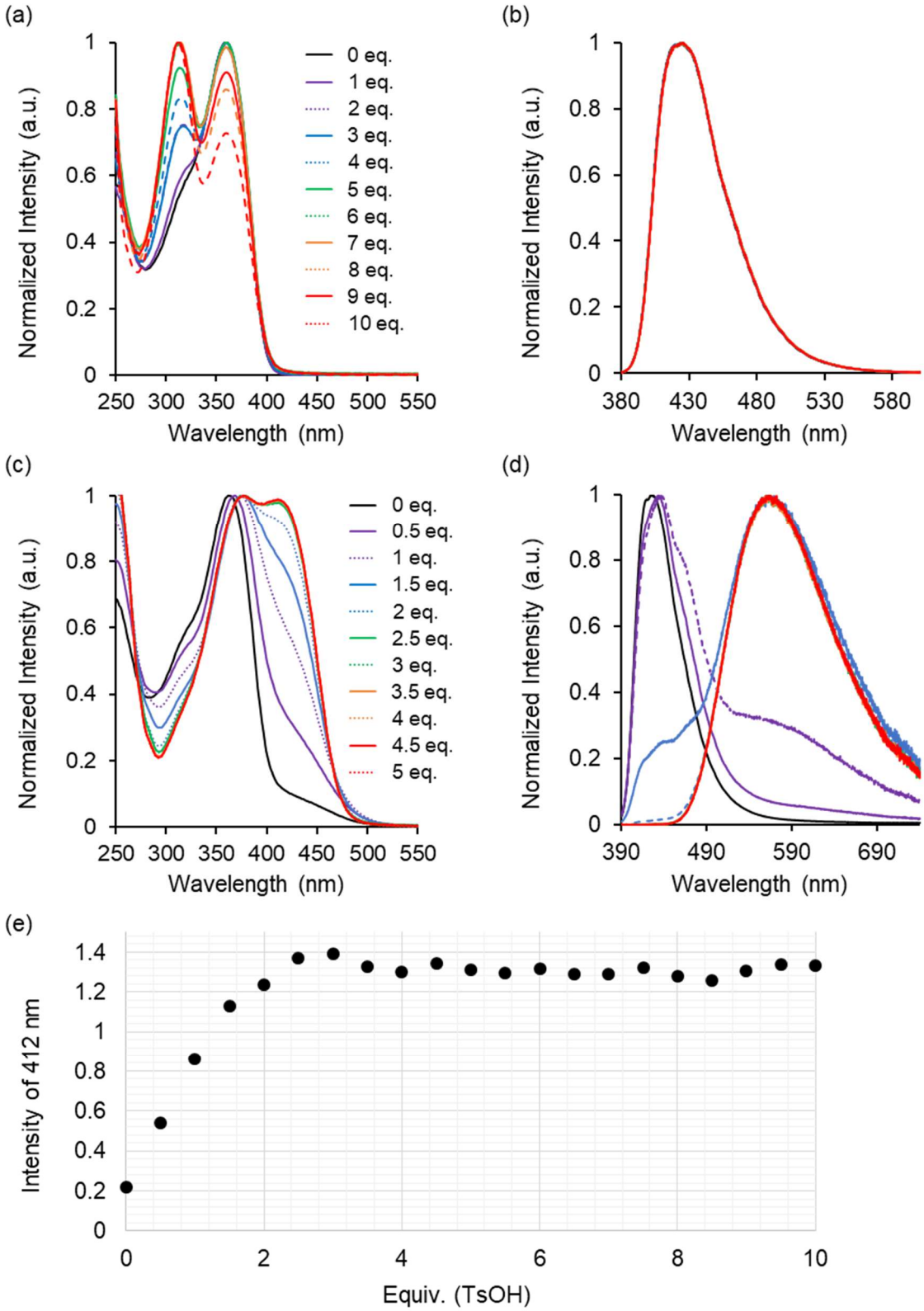

Fig. S29 (a) UV-vis spectra of mixture of **1** and **f** in CH_2Cl_2, (b) Emission spectra of mixture of **1** and **f** in CH_2Cl_2, (c) UV-vis spectra of mixture of **1** and **g** in $CHCl_3$ (d) Emission spectra of mixture of **1** and **g** in $CHCl_3$, (e) Relationship between emission intensity at 412 nm and equivalent of acid (**g**) to **1**.

DFT calculation

The geometry of 1 was optimized by performing DFT calculations using the B3LYP/6-31G(d) level of theory implemented in Gaussian 09.[1] The electronic excited states were calculated using the TD-DFT(B3LYP/6-31G(d)) method. Electron density difference maps (EDDM) were calculated by GAUSSSUM 3.0 program package[2] using results of TD-DFT. The calculated excited states are summarized in Tables S25. Representative molecular orbitals (MOs) are shown in Fig.s S27. The molecular orbitals involved in the dominant electron transitions and EDDM of the excited states for of **1** is shown in Fig.s S28. The results suggested that **1** showed intramolecular charge-transfer (ICT) character.

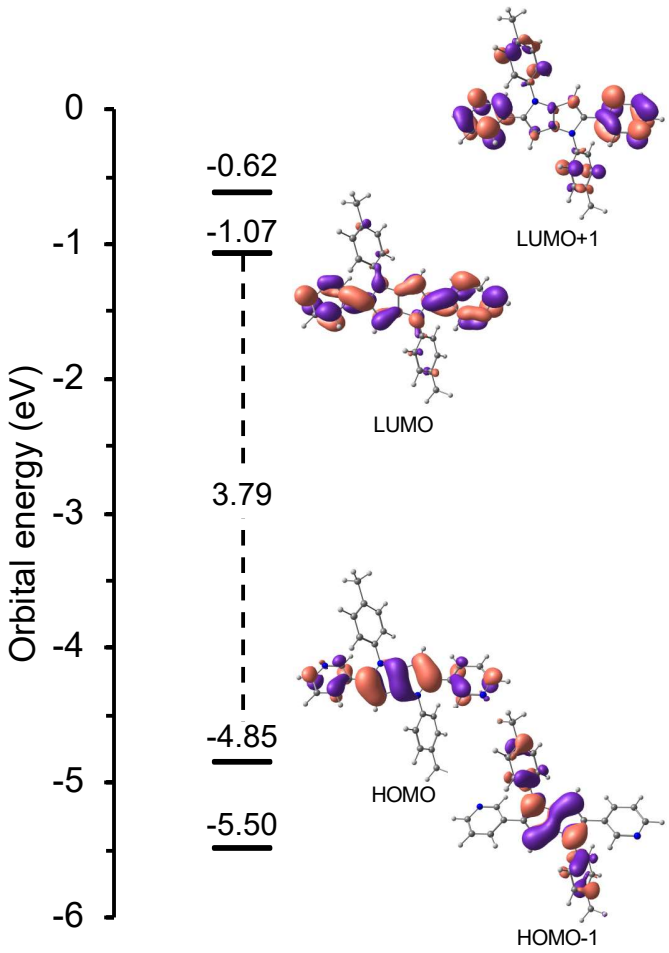

Fig. S30 Molecular orbital of **1**.

Table S25 Low-lying spin-singlet excited states of the **1** calculated using the B3LYP/6-31G(d) method.

State	ΔE (eV)	λ (nm)	f	Configuration		
				Occ. MO	Unocc. MO	Coeff
Trans. 1	3.4539	359	0.8284	116 →	117	0.69358
				116 →	119	-0.11480
Trans. 3	3.7953	327	0.1137	116 →	117	0.11303
				116 →	119	0.69231
Trans. 4	3.9064	317	0.1405	115 →	117	0.69831

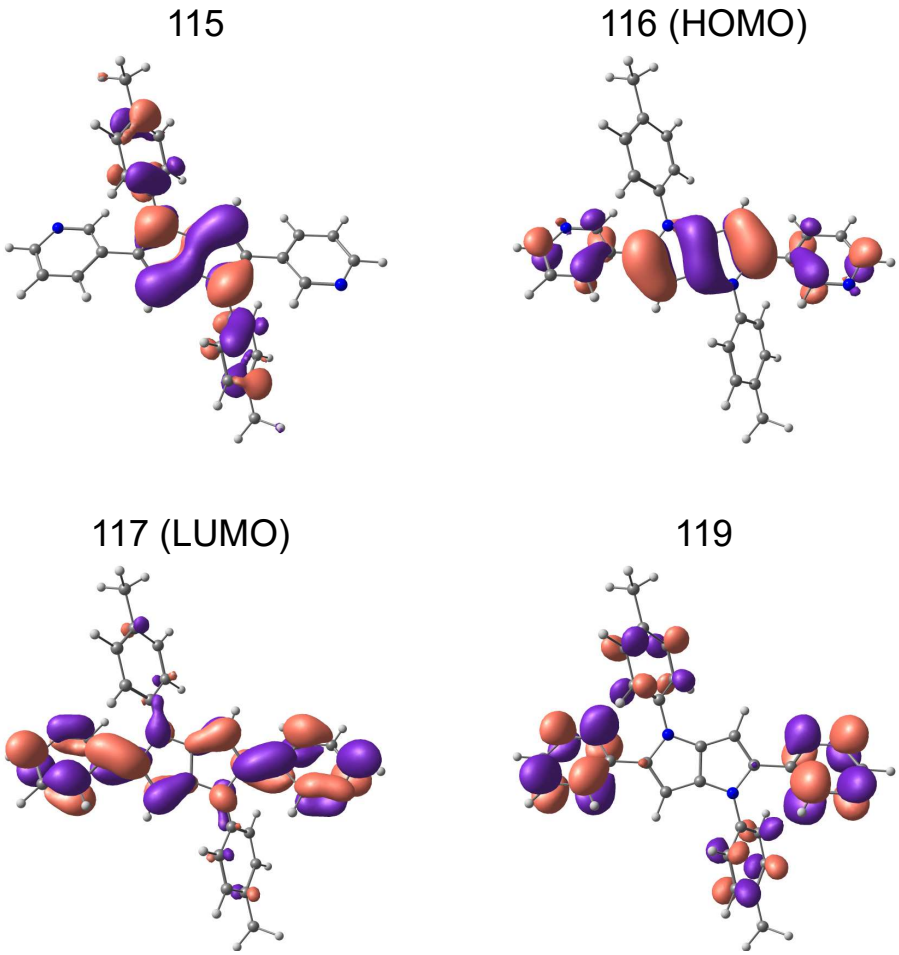

Fig. S31 Representative MOs of the **1**.

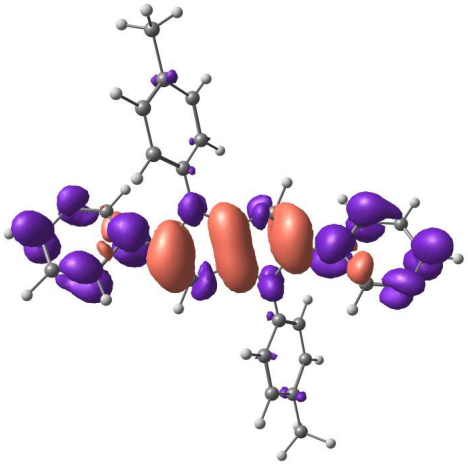

Transition 1

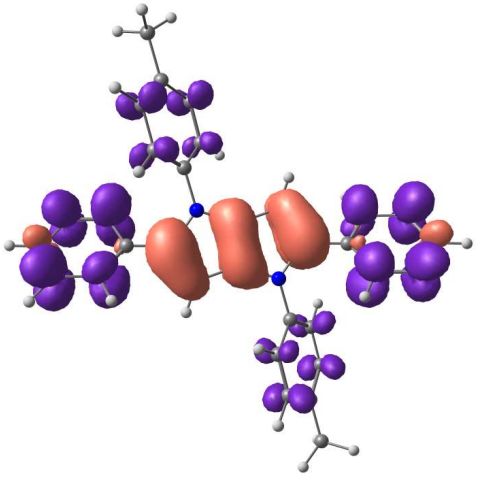

Transition 3

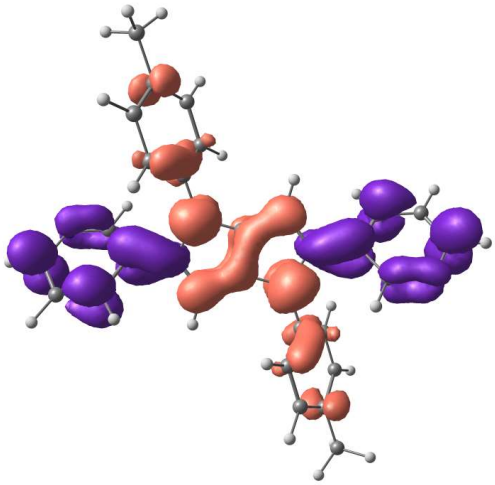

Transition 4

Fig. S32 Representative electron density difference maps (EDDM) between the electronic ground and excited states of **1**. The pink represents where the electrons are coming from, and the purple represents where the electrons are going.

Coordinates of the optimized structure of **1**

N	0.699703771	-0.166549545	1.579962914
N	3.413596172	-3.057495370	3.554177775
C	-0.187704135	0.275532740	0.611341135
C	2.681642789	-1.754005792	1.641154516
C	1.325654029	-1.091297211	-0.414397363
H	1.834549099	-1.724971869	-1.126517708
C	1.631703416	-1.008585150	0.942200272
C	0.747420911	0.357471390	2.903628020
C	4.886557208	-2.742785463	1.678925008
H	5.855028489	-2.929154027	1.223567800
C	1.925019882	0.908645904	3.421753206
H	2.821763521	0.930894580	2.811613859
C	-0.390573998	0.906424233	4.966089103
H	-1.301734524	0.902695613	5.559669795
C	1.936361410	1.434234104	4.710946705
H	2.859328475	1.857287523	5.100868903
C	3.924661948	-1.978891952	1.025794989
H	4.128648570	-1.543328275	0.051500249
C	0.782632762	1.444932512	5.507642676
C	2.493386585	-2.334747993	2.912150372
H	1.542869330	-2.214310982	3.426259373
C	-0.412904104	0.358977293	3.683729034
H	-1.325203598	-0.074639546	3.285241716
C	4.589275663	-3.253551545	2.942814410
H	5.321256765	-3.846883265	3.488270686
C	0.814816624	2.000370034	6.912167097
H	1.425076522	2.908642355	6.970517514
H	1.245507573	1.276366650	7.616515932
H	-0.190543530	2.245732273	7.269299985
N	-0.699703771	0.166549545	-1.579962914
N	-3.413596172	3.057495370	-3.554177775
C	0.187704135	-0.275532740	-0.611341135
C	-2.681642789	1.754005792	-1.641154516
C	-1.325654029	1.091297211	0.414397363

H	-1.834549099	1.724971869	1.126517708
C	-1.631703416	1.008585150	-0.942200272
C	-0.747420911	-0.357471390	-2.903628020
C	-4.886557208	2.742785463	-1.678925008
H	-5.855028489	2.929154027	-1.223567800
C	-1.925019882	-0.908645904	-3.421753206
H	-2.821763521	-0.930894580	-2.811613859
C	0.390573998	-0.906424233	-4.966089103
H	1.301734524	-0.902695613	-5.559669795
C	-1.936361410	-1.434234104	-4.710946705
H	-2.859328475	-1.857287523	-5.100868903
C	-3.924661948	1.978891952	-1.025794989
H	-4.128648570	1.543328275	-0.051500249
C	-0.782632762	-1.444932512	-5.507642676
C	-2.493386585	2.334747993	-2.912150372
H	-1.542869330	2.214310982	-3.426259373
C	0.412904104	-0.358977293	-3.683729034
H	1.325203598	0.074639546	-3.285241716
C	-4.589275663	3.253551545	-2.942814410
H	-5.321256765	3.846883265	-3.488270686
C	-0.814816624	-2.000370034	-6.912167097
H	-1.425076522	-2.908642355	-6.970517514
H	-1.245507573	-1.276366650	-7.616515932
H	0.190543530	-2.245732273	-7.269299985

1. Frisch, M. J.; Trucks, G. W.; Schlegel, H. B.; Scuseria, G. E.; Robb, M. A.; Cheeseman, J. R.; Scalmani, G.; Barone, V.; Mennucci, B.; Petersson, G. A.; Nakatsuji, H.; Caricato, M.; Li, X.; Hratchian, H. P.; Izmaylov, A. F.; Bloino, J.; Zheng, G.; Sonnenberg, J. L.; Hada, M.; Ehara, M.; Toyota, K.; Fukuda, R.; Hasegawa, J.; Ishida, M.; Nakajima, T.; Honda, Y.; Kitao, O.; Nakai, H.; Vreven, T.; Montgomery, J. A.; Peralta, J. E., Jr.; Ogliaro, F.; Bearpark, M.; Heyd, J. J.; Brothers, E.; Kudin, K. N.; Staroverov, V. N.; Kobayashi, R.; Normand, J.; Raghavachari, K.; Rendell, A.; Burant, J. C.; Iyengar, S. S.; Tomasi, J.; Cossi, M.; Rega, N.; Millam, J. M.; Klene, M.; Knox, J. E.; Cross, J. B.; Bakken, V.; Adamo, C.; Jaramillo, J.; Gomperts, R.; Stratmann, R. E.; Yazyev, O.; Austin, A. J.; Cammi, R.; Pomelli, C.; Ochterski, J. W.; Martin, R. L.; Morokuma, K.; Zakrzewski, V. G.; Voth, G. A.; Salvador, P.; Dannenberg, J. J.; Dapprich, S.; Daniels, A. D.; Farkas, O.; Foresman, J. B.; Ortiz, J. V.; Cioslowski, J.; Fox, D. J. Gaussian 09, revision D.01; Gaussian, Inc.: Wallingford, CT, **2009**.
2. O'Boyle, N. M.; Tenderholt, A. L.; and Langner. K. M.; *J. Comp. Chem.* **2008**, *29*, 839.